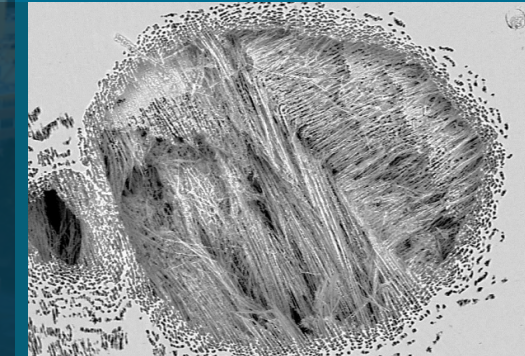
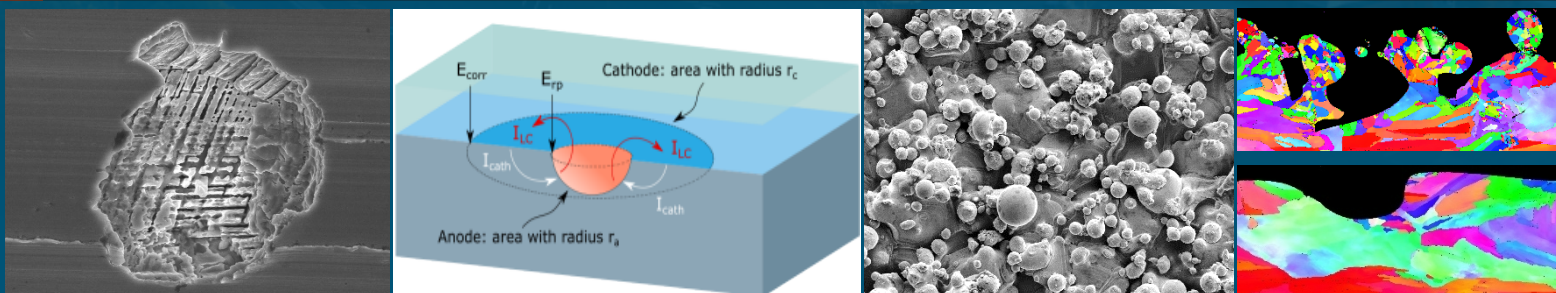




Additively manufactured stainless steel susceptibility to localized corrosion and stress corrosion cracking



PRESENTED BY

Presenter: Michael A. Melia

SNL: Jason Taylor, Jesse Duran, Erin Karasz, Rebecca Schaller,
Kyle Johnson, Philip Noell
DNV-GL: Ramgopal Thodla
OSU: Eric Schindelholz

Acknowledgements



Funding: Aging and Lifetime Program and the DoD-DOE Joint Munitions Program.

Many people to thank...

SNL: David Saiz, Bradley Jared, Philip Reu, Ryan Katona, Chuck Walker.

DNV-GL: Brandan Gerst.

OSU: Prof. Jen Warner.

Thanks to the symposium organizers for this opportunity.

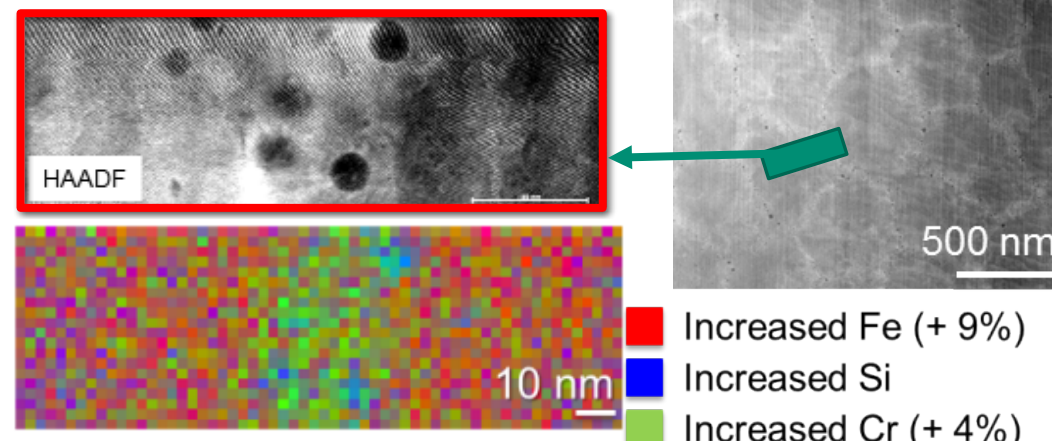
Microstructural features and processing defects

Chemical heterogeneities



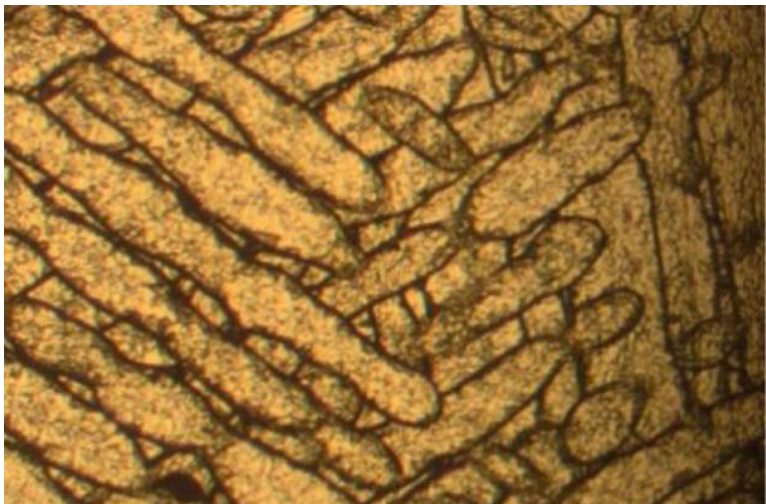
Cell walls decorated with oxides

Matrix Cell Boundary Matrix



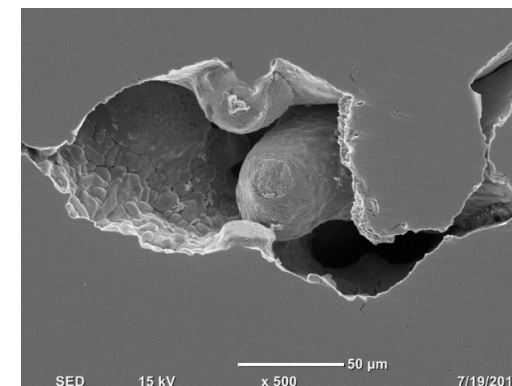
Melt pool interfaces

Schaller, 2018



SLM 316L (Macatangay et al. 2018)

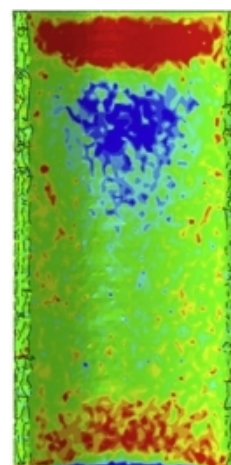
Porosity



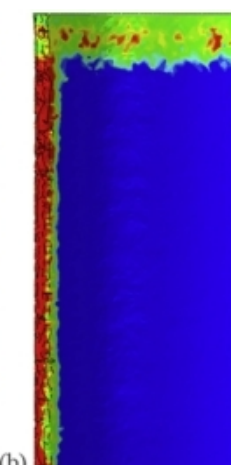
Melia, 2019

Residual stress

Hoop stress

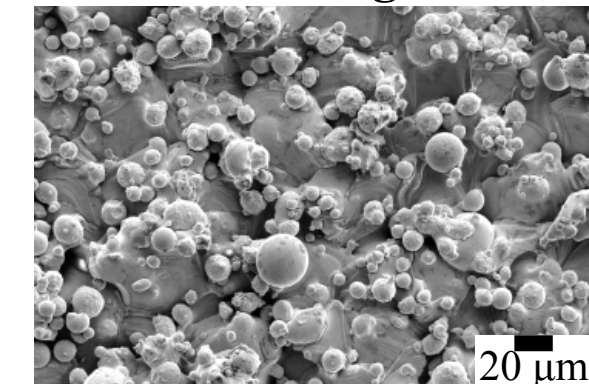


Axial stress



Processing defects

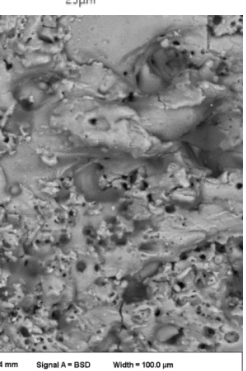
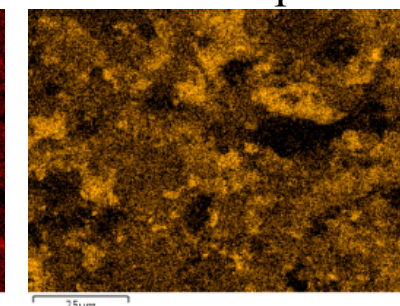
Surface roughness



Melia, 2020

Recast layer from wire EDM part removal

Zn map



Cu map

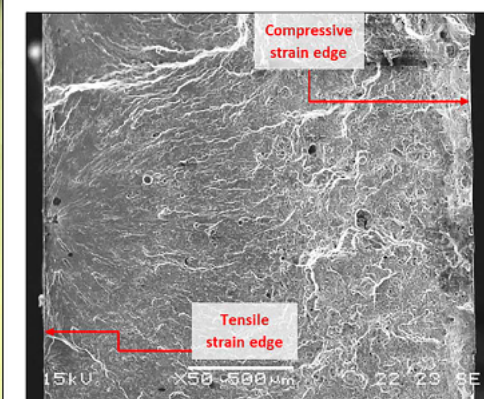
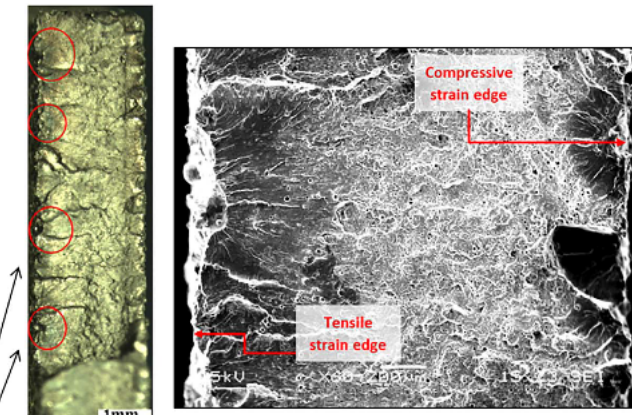
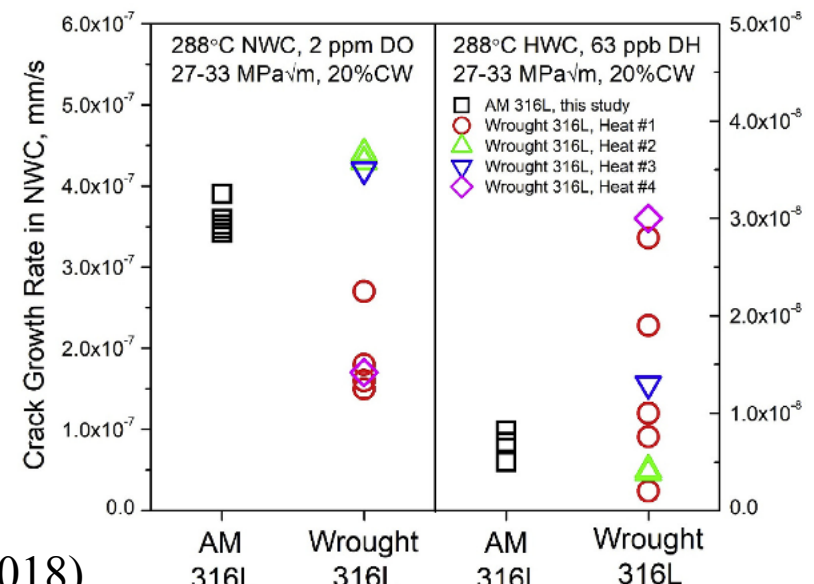
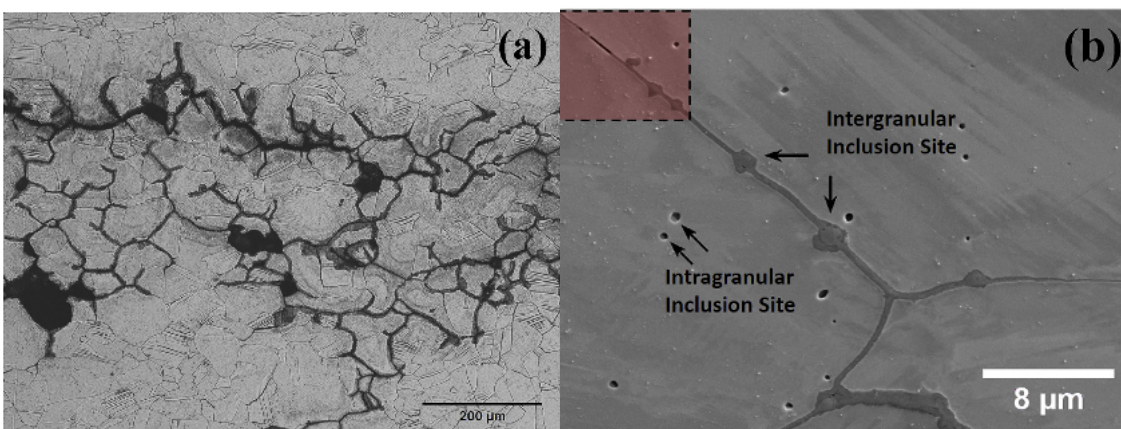
What needs understanding for SCC of AM stainless steels



Differences from wrought materials:

- Melt pool boundaries.
- Nanoscale non-metallic inclusions.
- High dislocation density.
 - Not from cold working.
 - Cellular structure.
- Sub-grain boundaries.

(Lou et al. 2018)



(Leon et al. 2017)

Work on AM Al alloy (AlSi10Mg) showed as-printed surface roughness leads to initiation of numerous SCC sites in aerated 0.6 M NaCl.

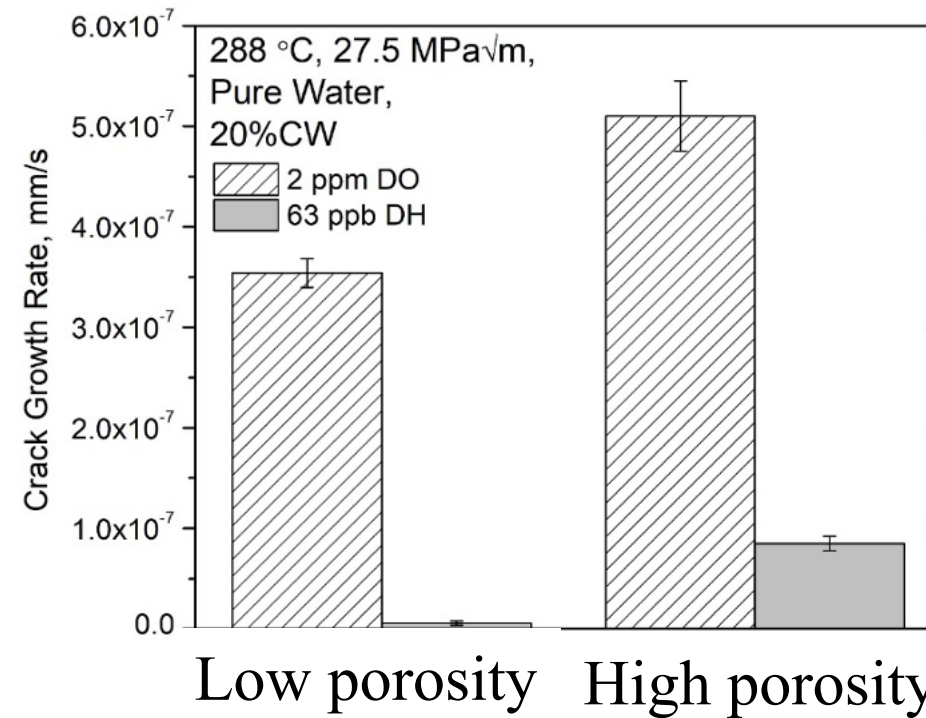
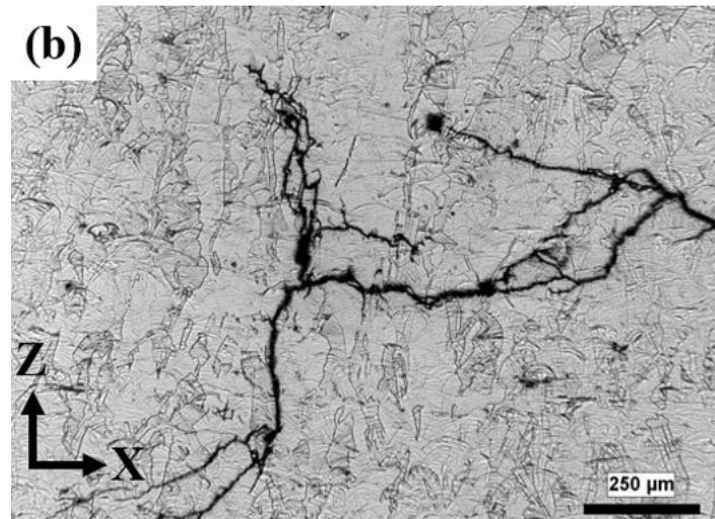
Polished AM Ni alloy (625) showed minimal difference in SCC behavior in quiescent 0.6 M NaCl.

Studies to date AM environmental assisted cracking

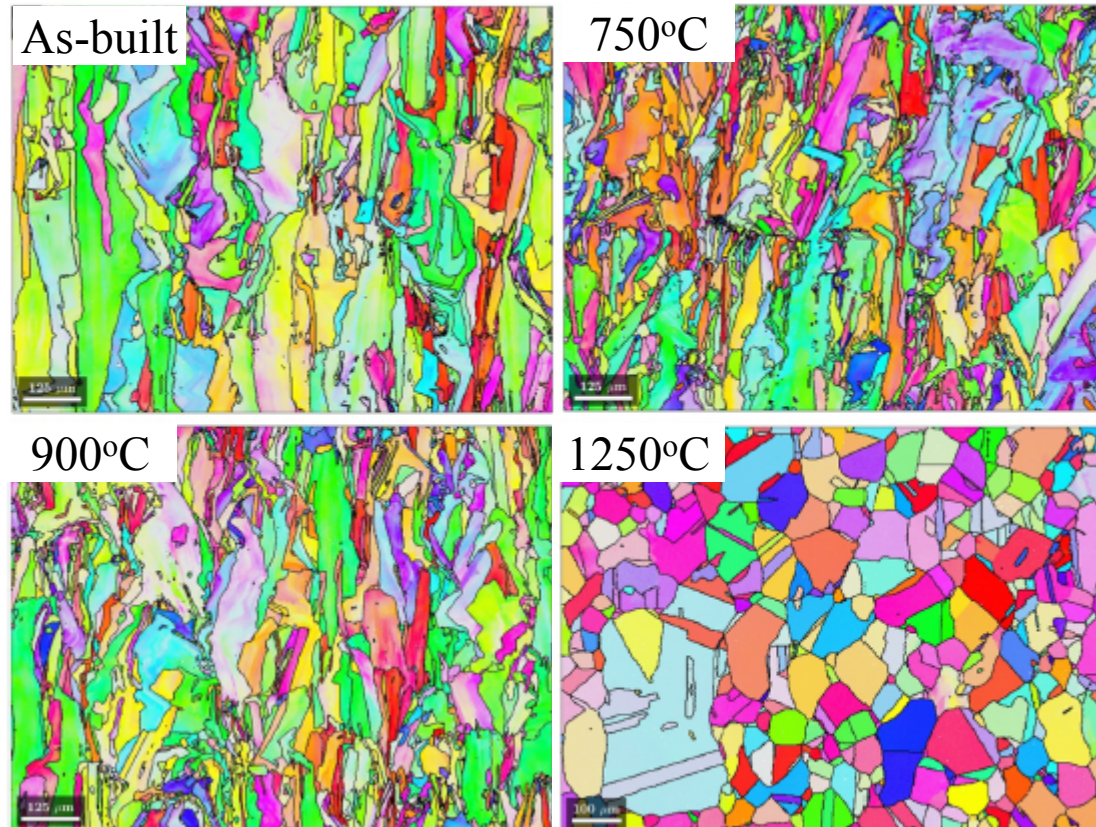


Luo, 2017; **SLM 316L in boiling water reactor conditions:**

- Differences in crack propagation depending on build orientation, columnar grains caused more tortuous path.
 - Subgrain deformation structures appear to be driving force for SCC.
- Hot isostatic pressing (HIP) and solution anneal (SA) led to similar results to wrought material.
- Porosity generally increases crack growth rate.
- Oxide inclusions helped propagate cracks along grain boundaries.

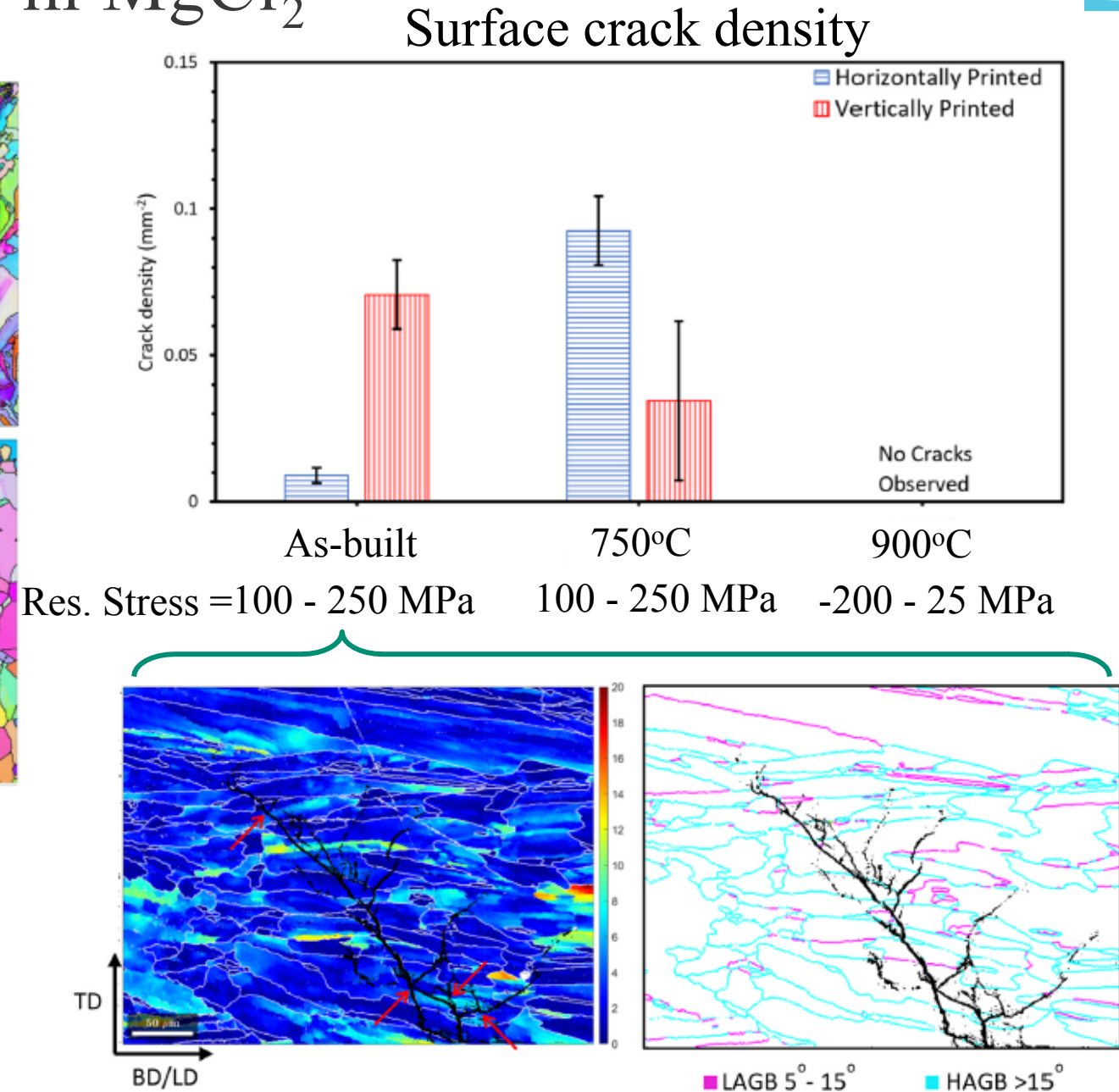


SCC of AM stainless steel in $MgCl_2$



SCC of powder bed fusion 316L material printed in vertical/horizontal orientations.

P. Dong, et al., Addit. Manuf., 40 (2021).



Study Framework



Questions

- 1) How does residual stress from PBF 316L specimens impact SCC behavior compared to conventional wrought material?
 - What heat treatments impact this SCC behavior?
- 2) What is the interplay of unique microstructural features with crack propagation?

Approach

Control residual stress of powder bed fusion specimen with cutting/heat treatments.

- Boiling $MgCl_2$ exposures.

Direct current potential drop (DCPD) SCC measurements.

- Crack growth rate measurements.
- Frequency dependence.

Study Framework

Questions



- 1) How does residual stress from PBF 316L specimens impact SCC behavior compared to conventional wrought material?
 - What heat treatments impact this SCC behavior?
- 2) What is the interplay of unique microstructural features with crack propagation?

Approach

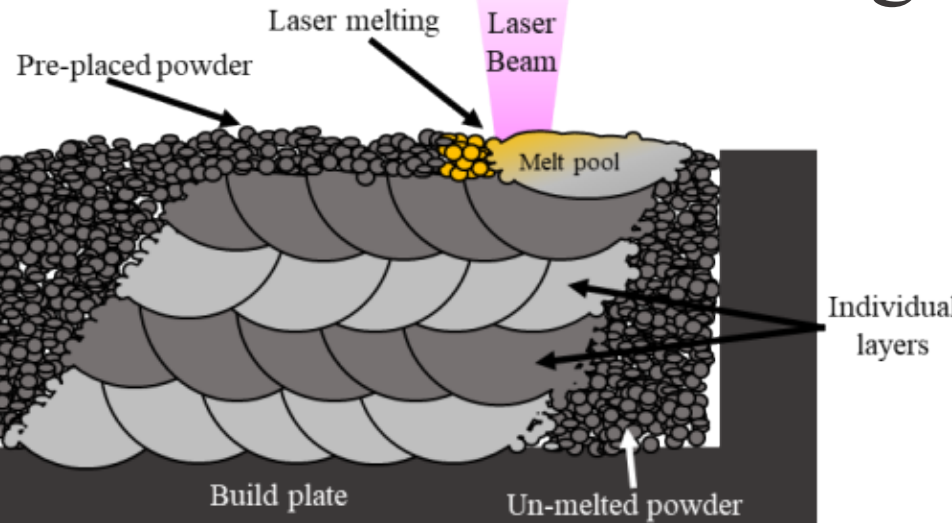
Control residual stress of powder bed fusion specimen with cutting/heat treatments.

- **Boiling MgCl₂ exposures.**

Direct current potential drop (DCPD) SCC measurements.

- Crack growth rate measurements.
- Frequency dependence.

Selective laser melting 316L samples



Parameter	Value
Laser power	110 W
Laser velocity	1400 mm/sec
Layer thickness	30 μ m
Laser focus offset	+1 mm
Average powder diameter	12 μ m
Cover gas	Argon

- Two batches of 25, 1.5 cm, cubes fabricated with different porosity levels.
- 5 different cut heights to produce specimens with significantly different residual stresses.**
- Density measurements: “Good batch, ~100%”, “Porous batch, ~96.4%”

Dense

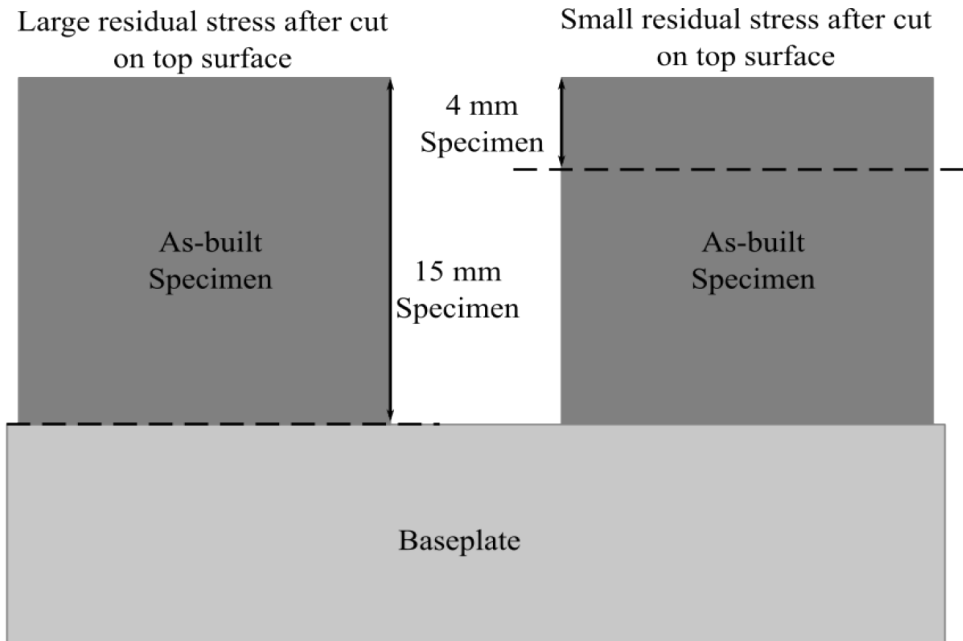


Porous

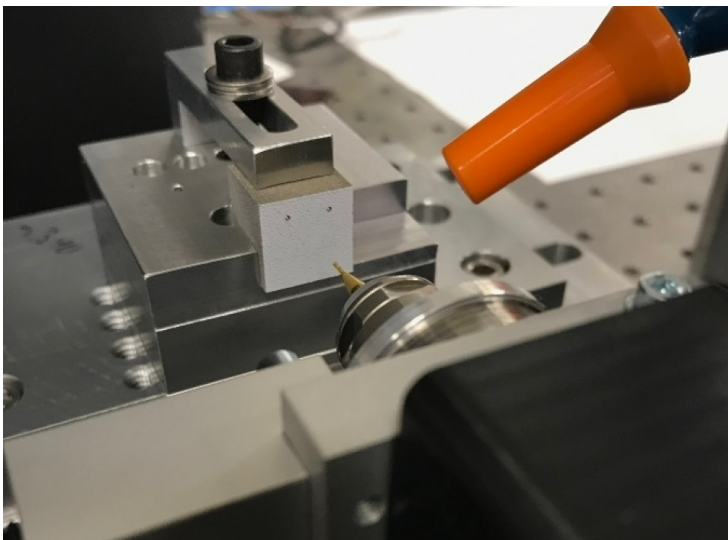


wt%	C	Cr	Cu	Fe	Mn	Mo	N	Nb	Ni	O	P	S	Si	PREN
316L wrought	0.012	16.76	0.56	68.4	1.25	1.91	0.056	0.021	10.14	0.003	0.029	0.002	0.22	24.0
316L SLM as-built	0.013	16.87	0.039	65.5	1.54	2.31	0.078	0.001	12.74	0.055	0.015	0.006	0.71	25.7

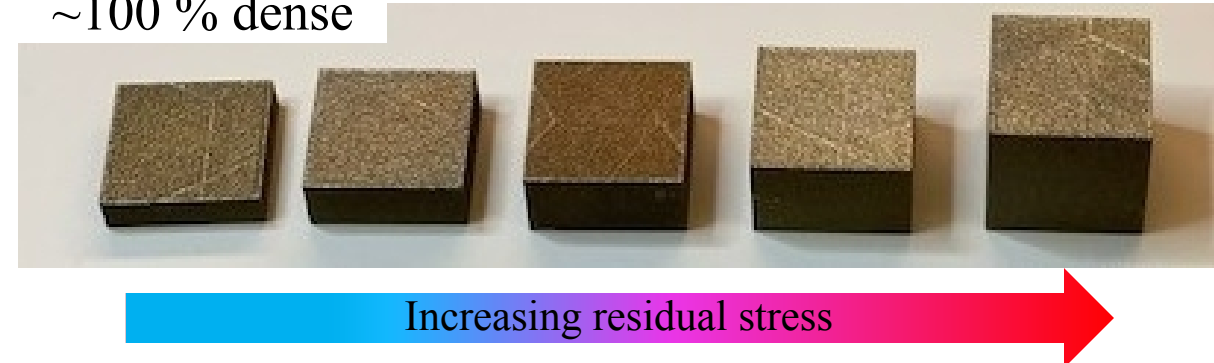
Control residual stress – maintain microstructure



Hole drilling used to measure σ_{xx} and σ_{yy}



~100 % dense



Res. Stress (MPa)

15 mm	σ_{xx} MPa	355
	σ_{yy} MPa	262
10 mm	σ_{xx} MPa	260
	σ_{yy} MPa	158
8 mm	σ_{xx} MPa	190
	σ_{yy} MPa	115
6 mm	σ_{xx} MPa	165
	σ_{yy} MPa	106

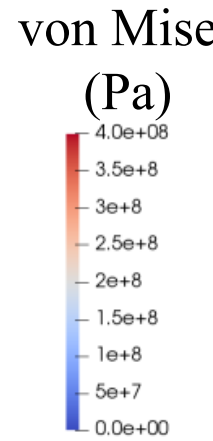
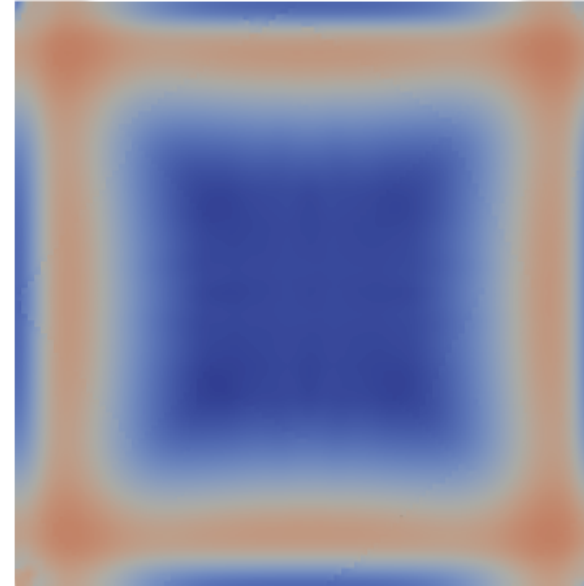
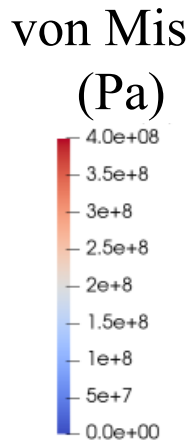
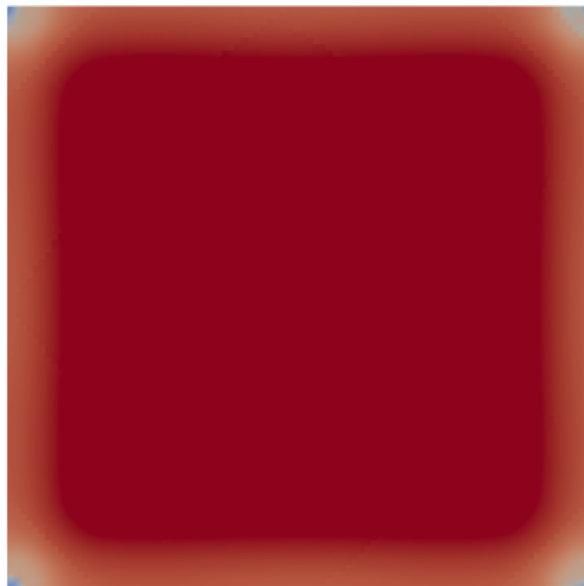
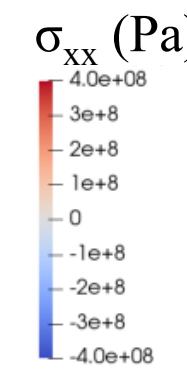
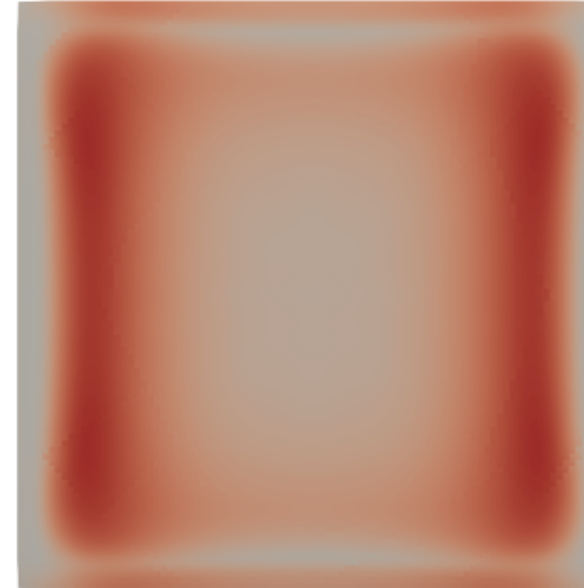
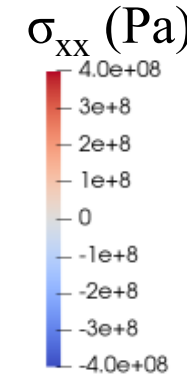
Control residual stress are expected by simulations



15 mm tall

4 mm tall

Build
direction



Average VM Stress
in dark red region =
+430 MPa

Boiling MgCl₂ experiments

~100 % dense



All sides of sample, except top surface,
were coated with epoxy

ASTM G36-94: Standard Practice for Evaluating Stress-Corrosion-Cracking Resistance of Metals and Alloys in a Boiling Magnesium Chloride Solution

Prepared about 400 mL of the test solution for use in the boiling vessel.

- 600 g of reagent grade MgCl₂·6H₂O
- 15 mL of reagent water

Solution held to boil at ~155 °C for at least 24 hours (some samples were in for longer if no cracking was observed).

Condenser



Thermometer

Vessel

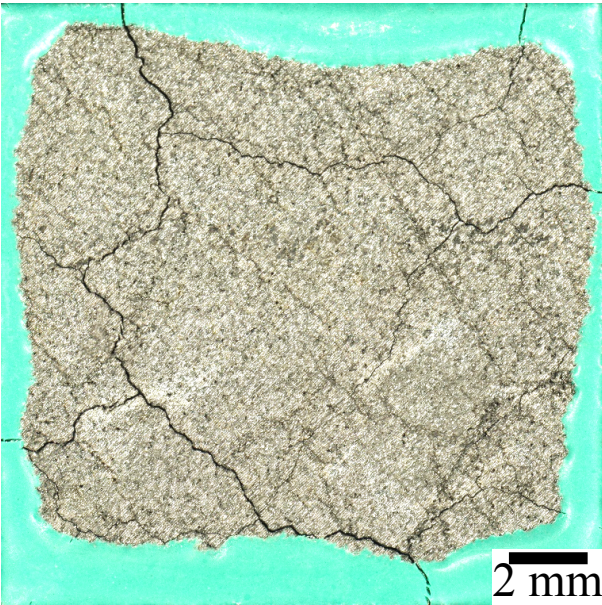
Heating jacket

Thermocouple control

Cube sample exposure to boiling MgCl₂



15 mm tall



4 mm tall



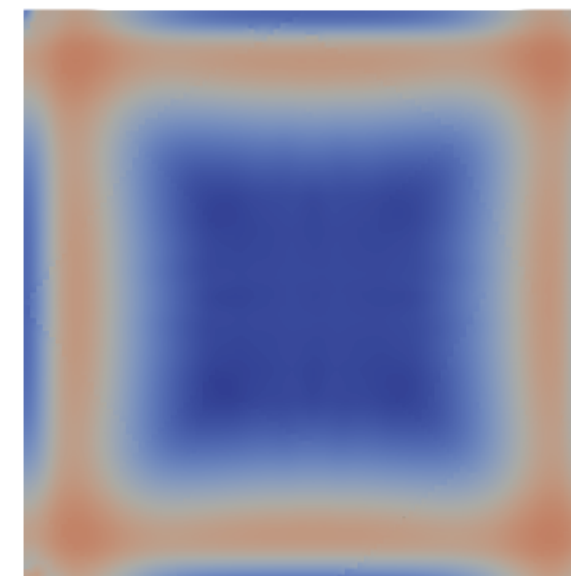
Boiling MgCl₂ at 155 °C, imaged after 24 hours.

Average VM Stress
in dark red region =
+430 MPa



von Mises (Pa)

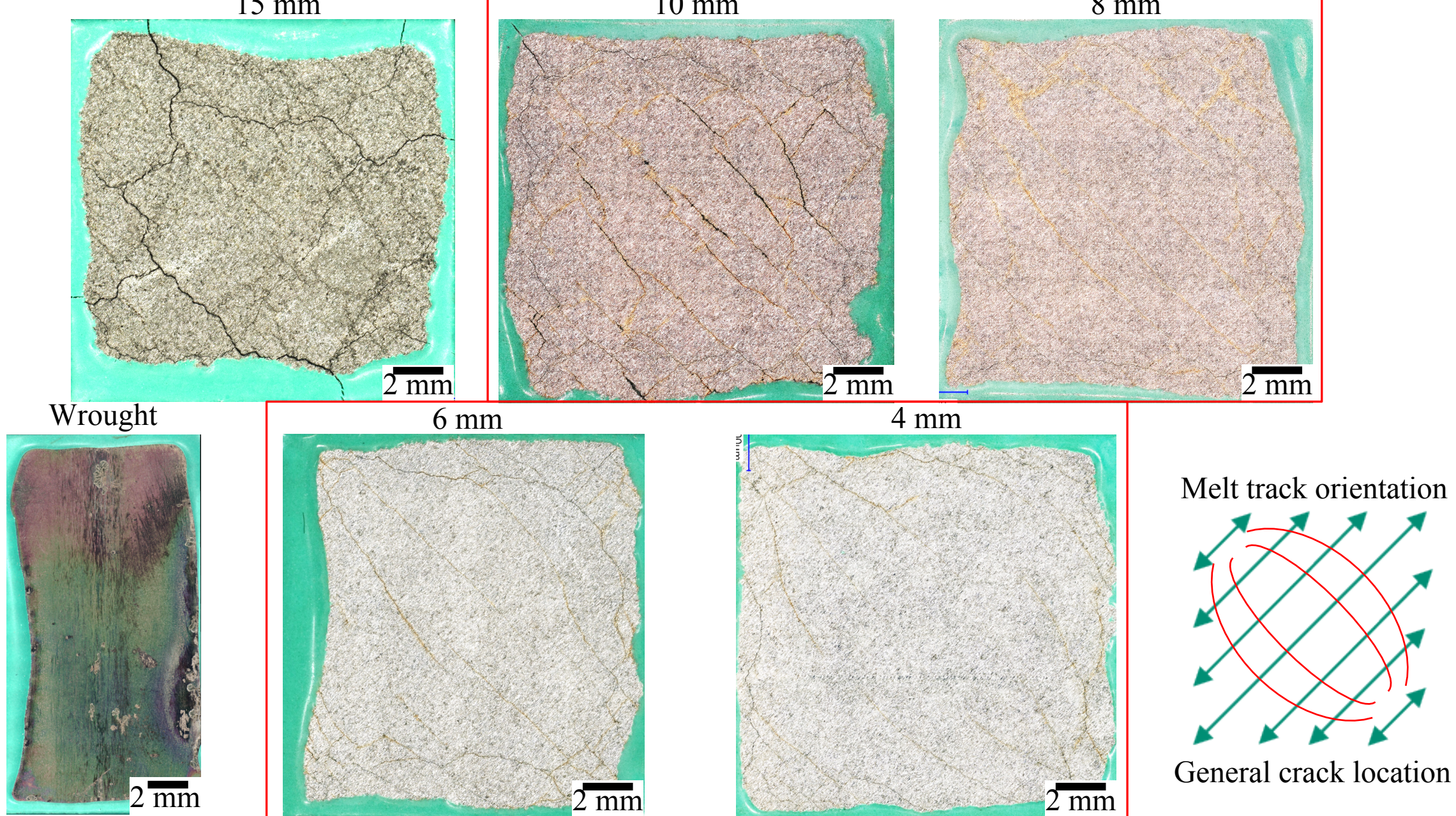
4.0e+08
3.5e+08
3e+08
2.5e+08
2e+08
1.5e+08
1e+08
5e+07
0.0e+00



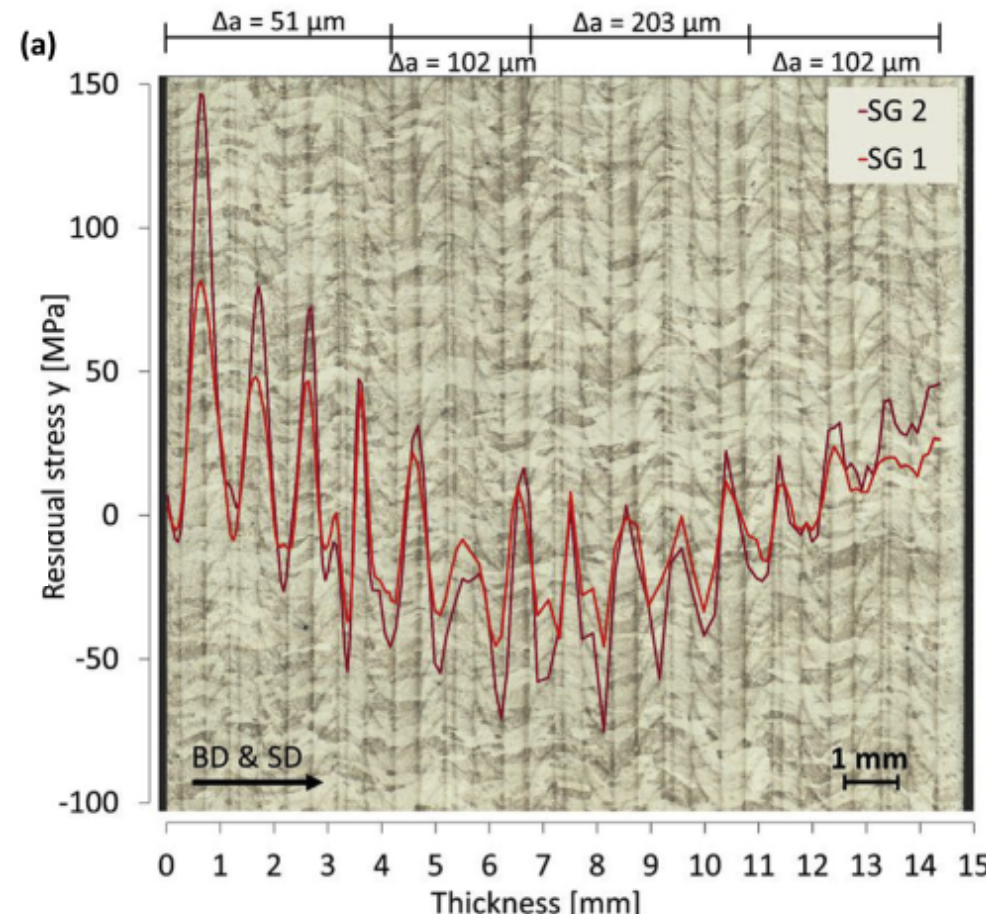
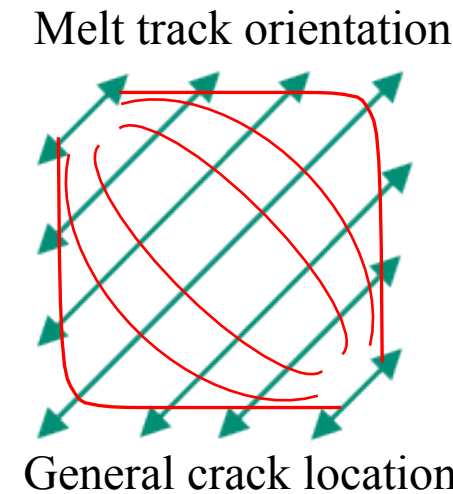
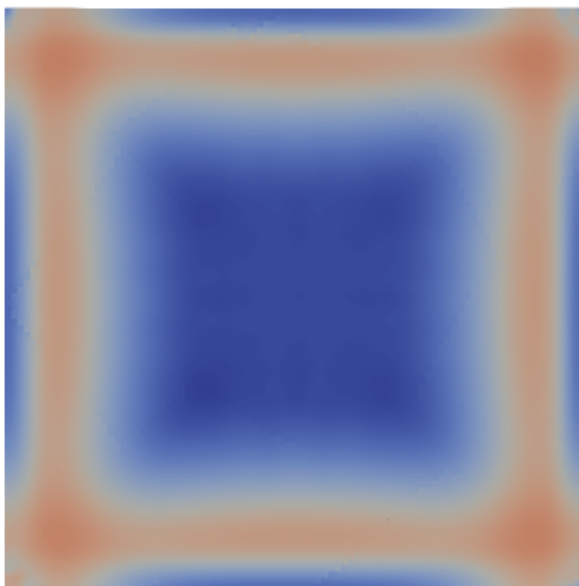
von Mises (Pa)

4.0e+08
3.5e+08
3e+08
2.5e+08
2e+08
1.5e+08
1e+08
5e+07
0.0e+00

Cube sample exposure to boiling $MgCl_2$



Impact of the final layer

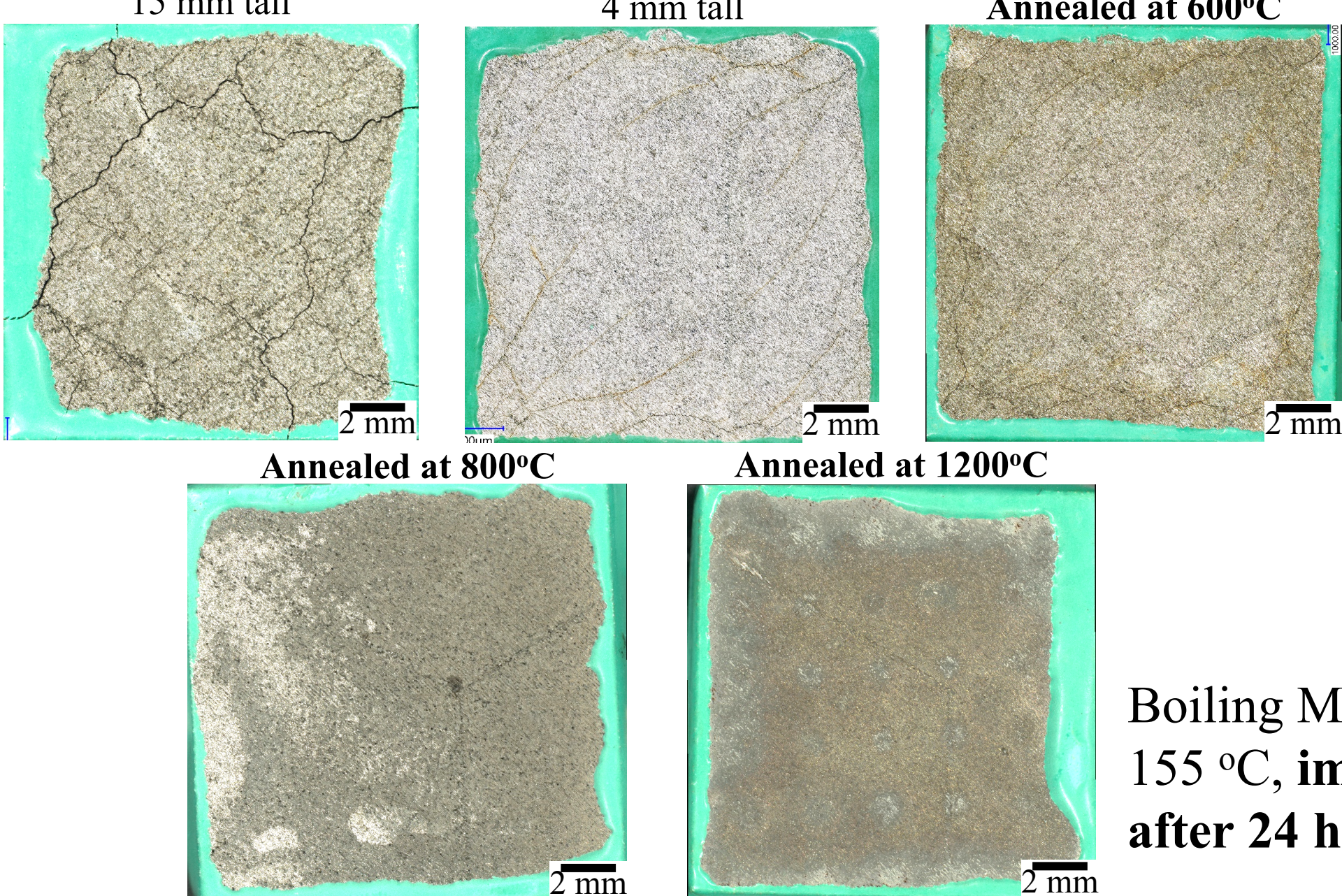


M. Strantza, et al., Acta Mater. (2019).

Strantza et al. have shown each layer of deposited material can have fluctuations in residual stress state.

There is still a macro-scale change in the stress state.

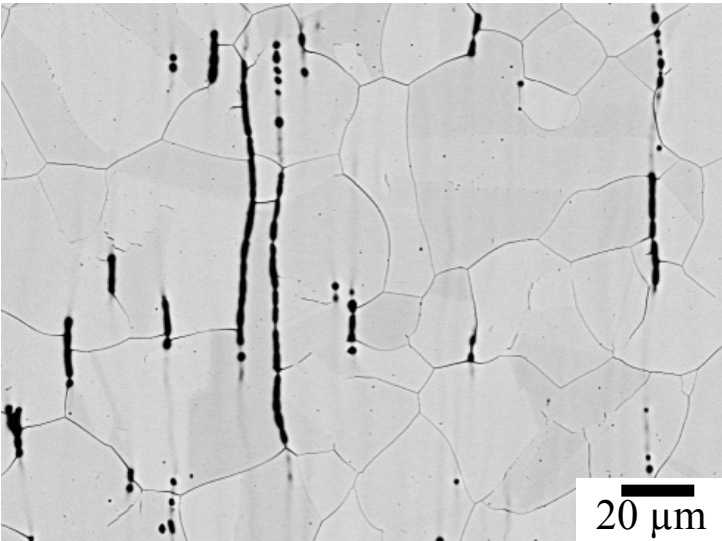
Cube sample exposure to boiling MgCl_2



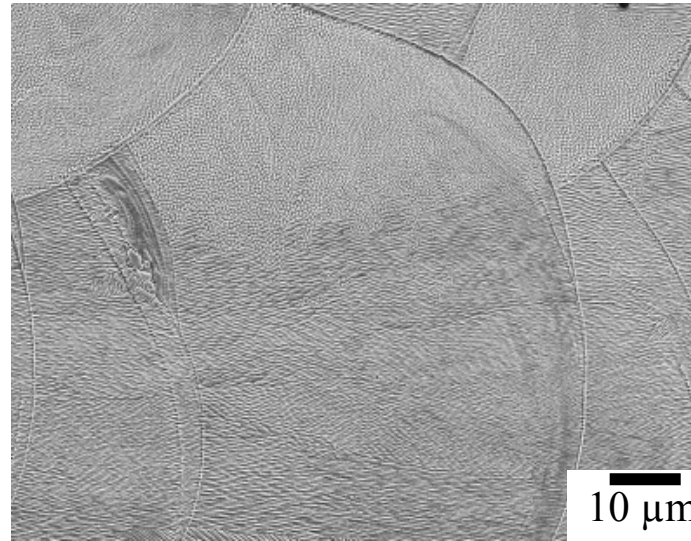
Boiling MgCl_2 at
155 °C, imaged
after 24 hours.

Etched microstructure – SEM imaging

Wrought

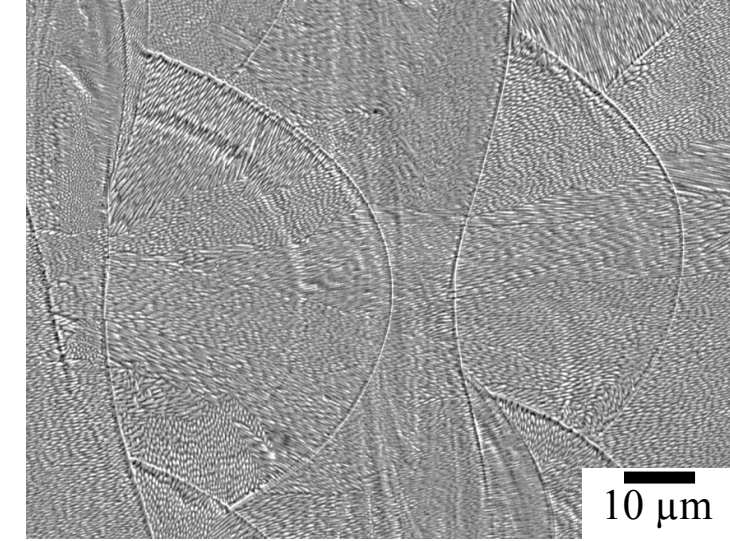


As-printed

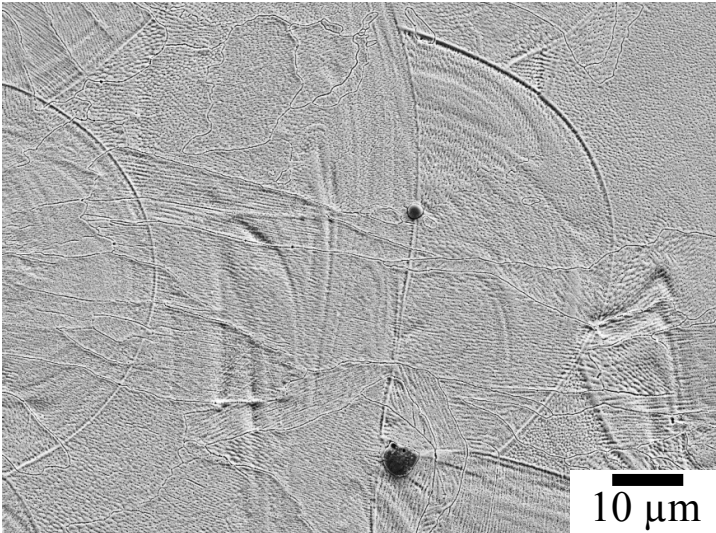


PBF

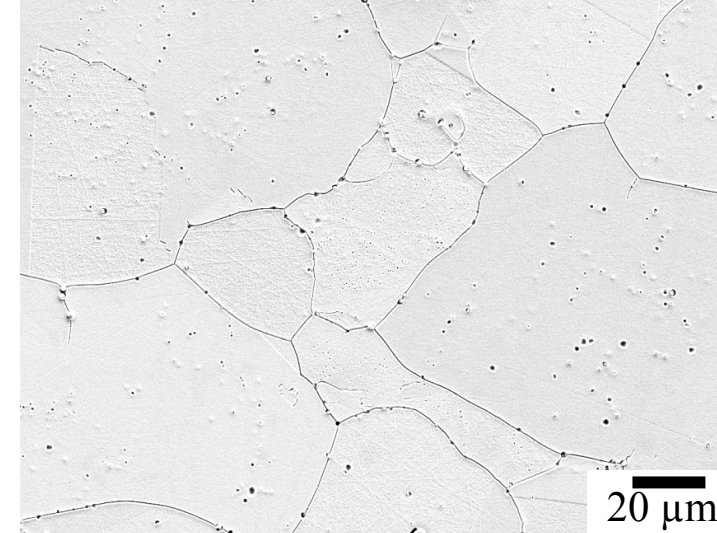
600°C



800°C



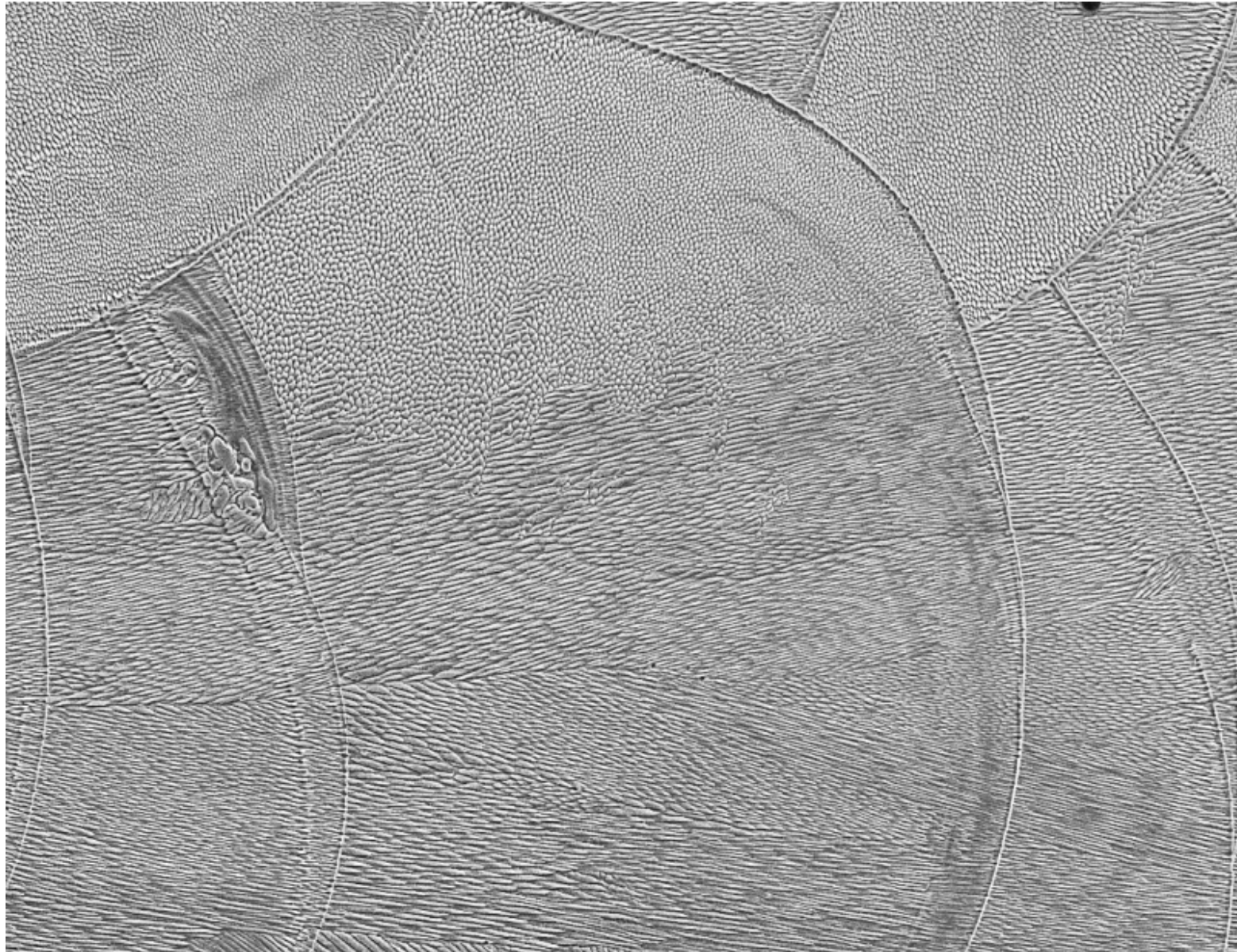
1200°C



Etched microstructure – SEM imaging

18

As-printed

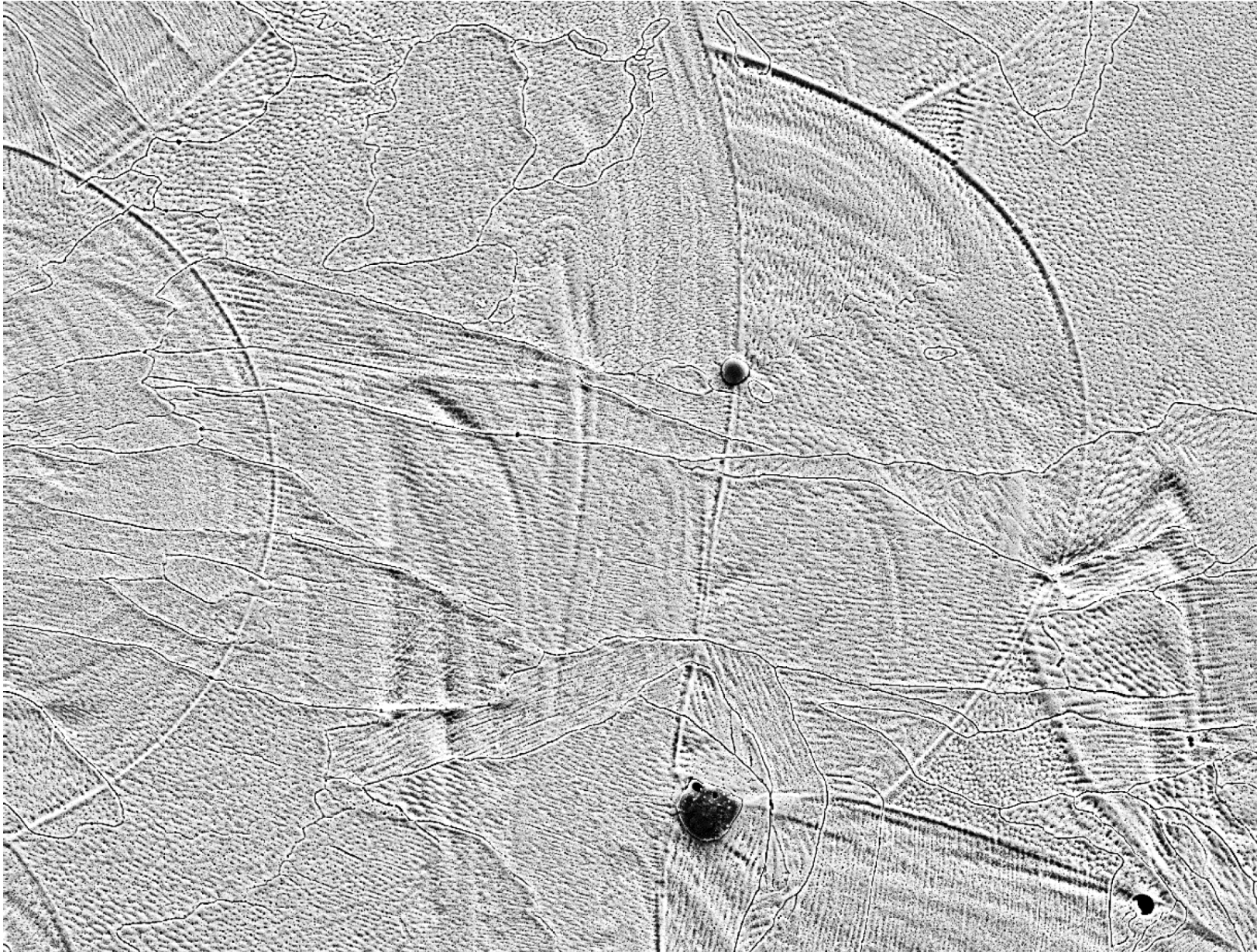


Etched microstructure – SEM imaging

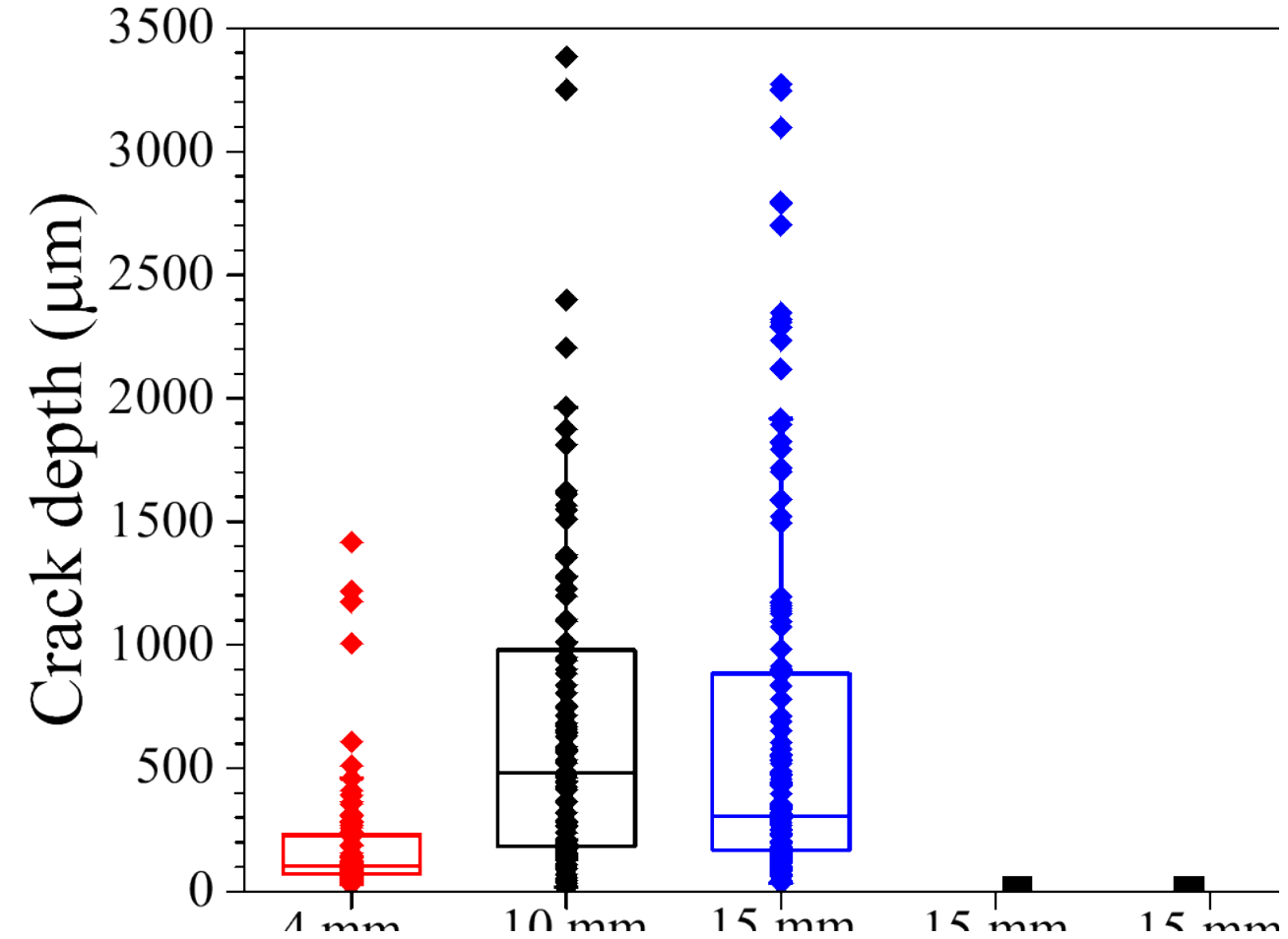
800°C



On the cusp of
recrystallization



Cube sample exposure to boiling MgCl_2

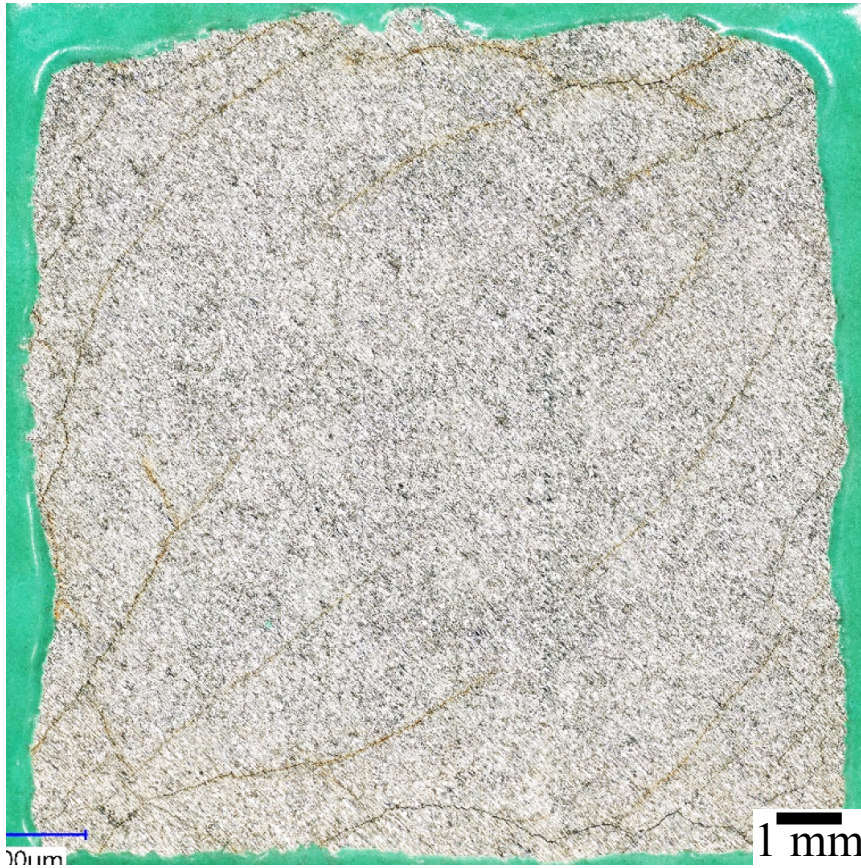


Boiling MgCl_2 at 155°C , imaged after 24 hours.

Impact of porosity?



Dense

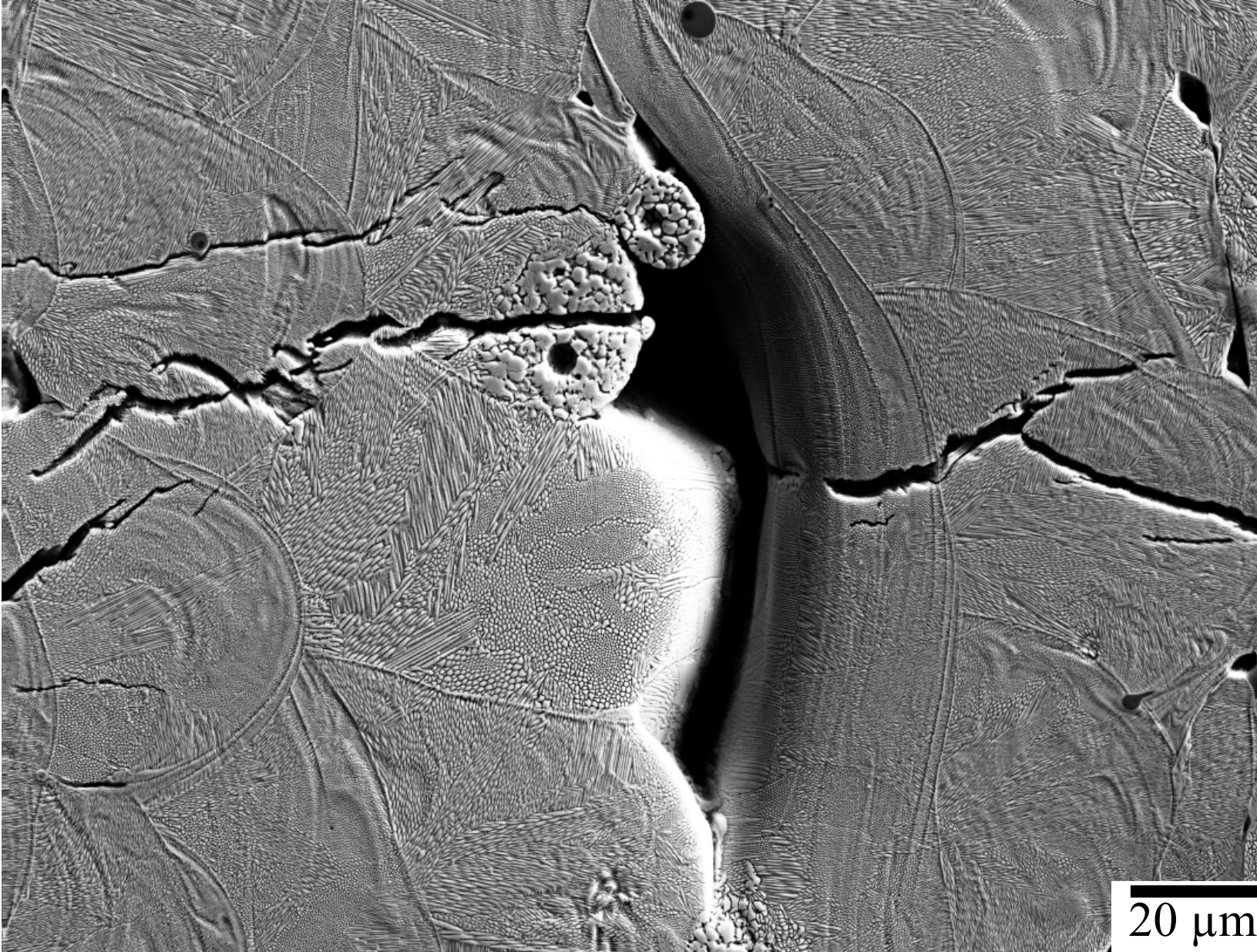


Porous (~ 5 vol%)



Impact of porosity?

22



Conclusions from Boiling MgCl₂ experiments



Controlling residual stress with cutting.

- Residual stress was simulated to be a maximum at 430 MPa for thickest sample.
- Samples with lower global residual stress showed crack propagation perpendicular to the melt track directions.

Annealing study.

- Heat treated samples at 600, 800, and 1200°C for 1 hour.
- 600°C stress relief has minimal impact on crack susceptibility or propagation depth.
- Cracking was non-existence for annealed 800 and 1200°C samples.
 - 800°C sample showed the beginnings of recovery and recrystallization which seemed to be enough to prevent cracking after >300 hrs. immersion.

Porosity might reduce SCC susceptibility.

Study Framework

Questions

- 1) How does residual stress from PBF 316L specimens impact SCC behavior compared to conventional wrought material?
 - What heat treatments impact this SCC behavior?

- 2) What is the interplay of unique microstructural features with crack propagation?

Approach

Control residual stress of powder bed fusion specimen with cutting/heat treatments.

- Boiling $MgCl_2$ exposures.

Direct current potential drop (DCPD) SCC measurements.

- **Crack growth rate measurements.**
- **Frequency dependence.**

Preliminary data

Crack growth rate measurements



Environment

- Immersed in saturated MgCl_2 .
- Temperature kept at 75°C.

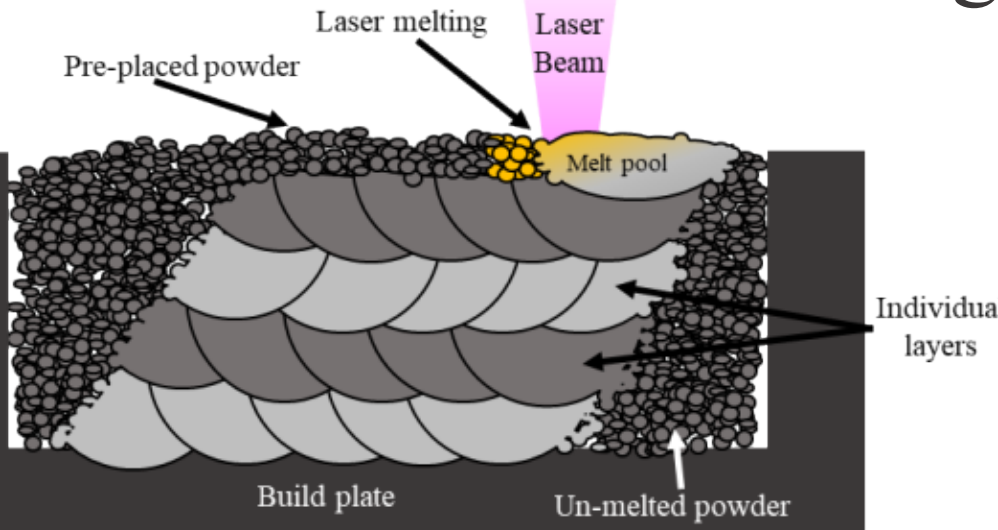
Sample (3/4 CT) – coated on all sides except the crack flanks/crack notch.

- Wrought samples were prepared in as-received condition.
- PBF 316L samples were prepared in as-printed, annealed (650 and 1200 °C) conditions.

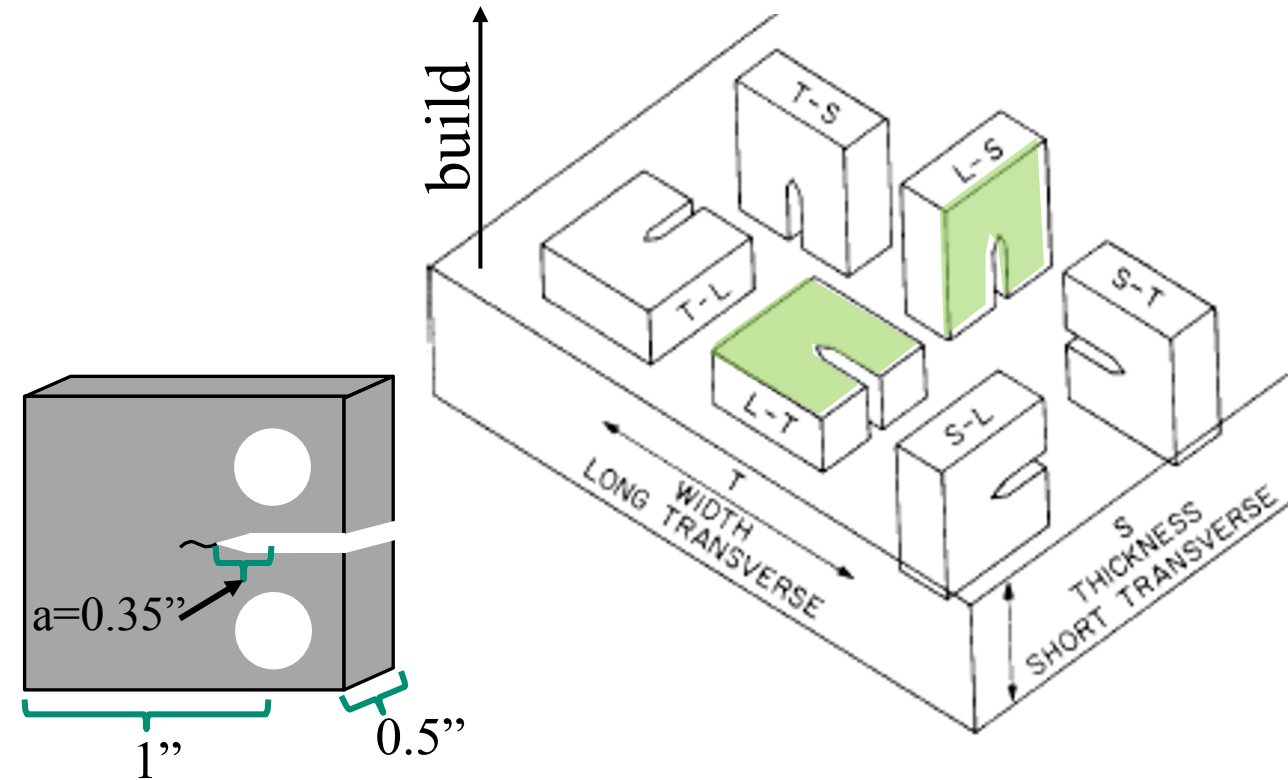
Loading conditions

- $K_{\max} = 44 \text{ MPa}\sqrt{\text{m}}$.
- $R = 0.5$.
- Freq: 0.1Hz to 1mHz
 - 9000s holds
 - 1 day holds
 - and transitioned to constant K .

Selective laser melting 316L samples



Parameter	Value
Laser power	110 W
Laser velocity	1400 mm/sec
Layer thickness	30 μ m
Laser focus offset	+1 mm
Average powder diameter	12 μ m
Cover gas	Argon



Laser pattern turns 90 degrees every layer and the starting position changes every layer. Identical laser scan pattern occurs every 4th layer.

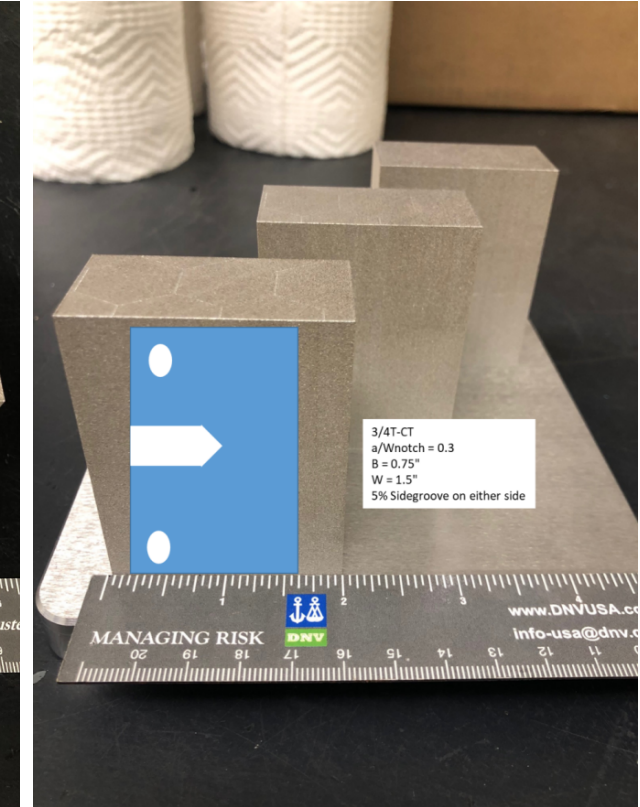
wt%	C	Cr	Cu	Fe	Mn	Mo	N	Nb	Ni	O	P	S	Si	PREN
316L wrought	0.012	16.76	0.56	68.4	1.25	1.91	0.056	0.021	10.14	0.003	0.029	0.002	0.22	24.0
316L SLM as-built	0.013	16.87	0.039	65.5	1.54	2.31	0.078	0.001	12.74	0.055	0.015	0.006	0.71	25.7

Materials

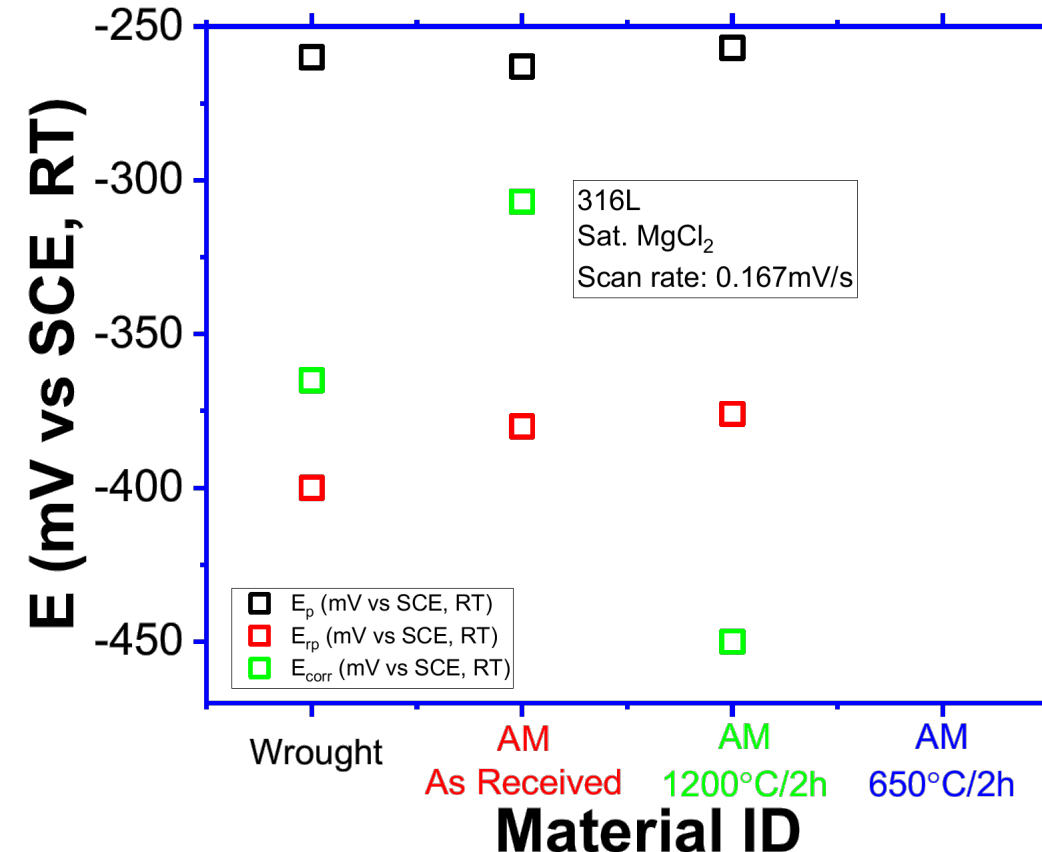
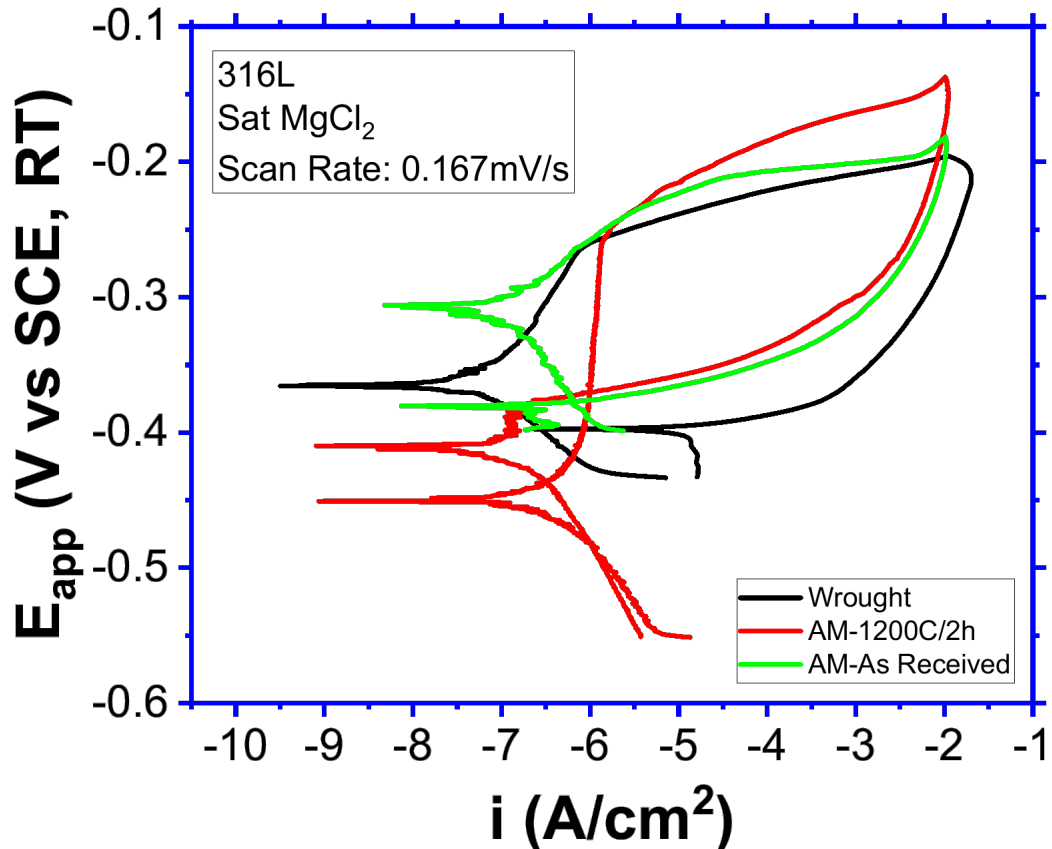
Wrought 316L



AM 316L blocks printed at SNL

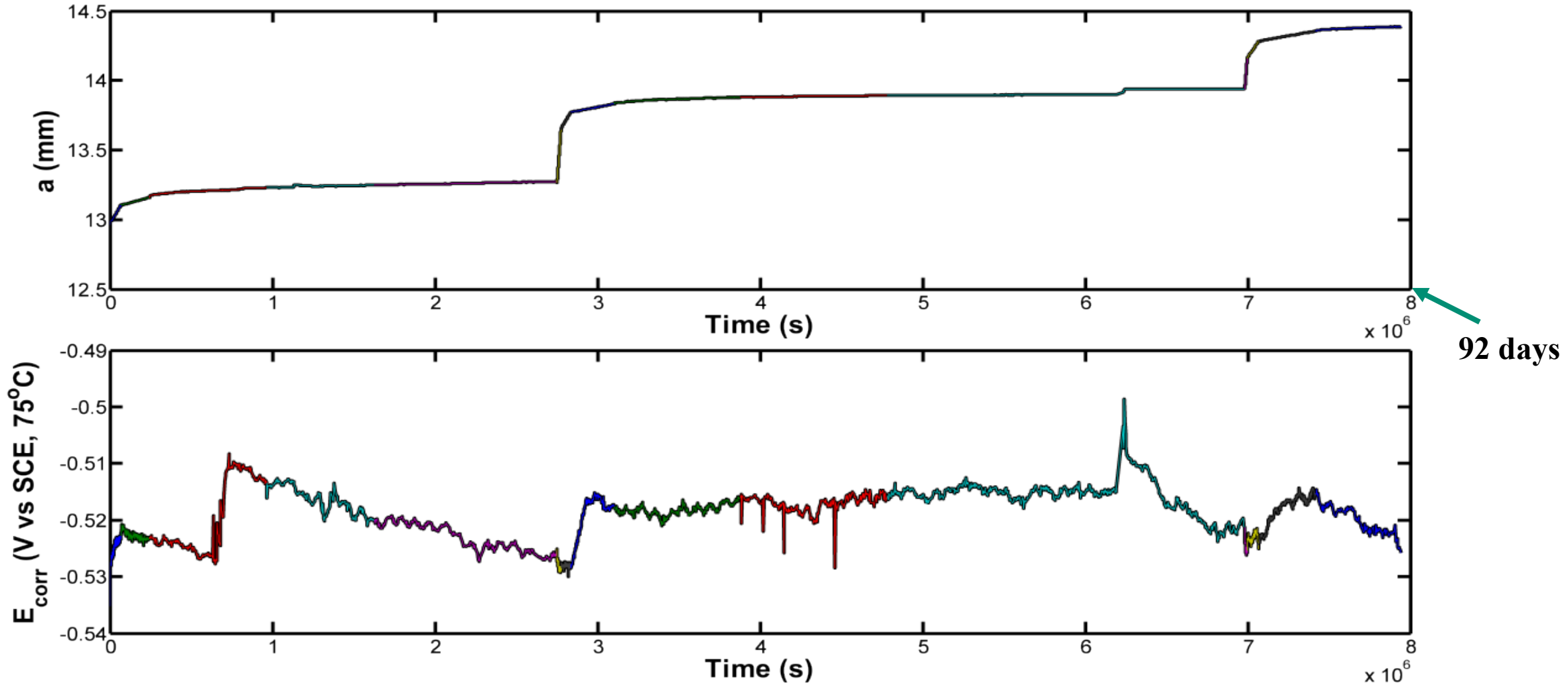


AM Sample Electrochemical Tests



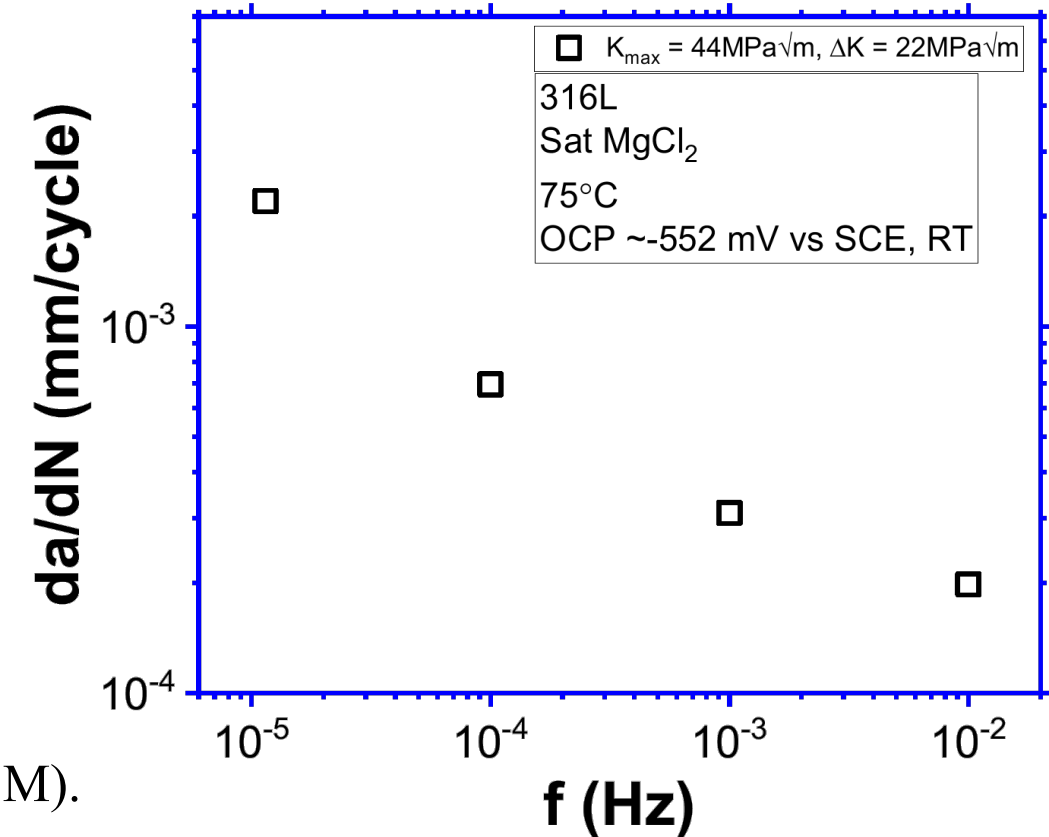
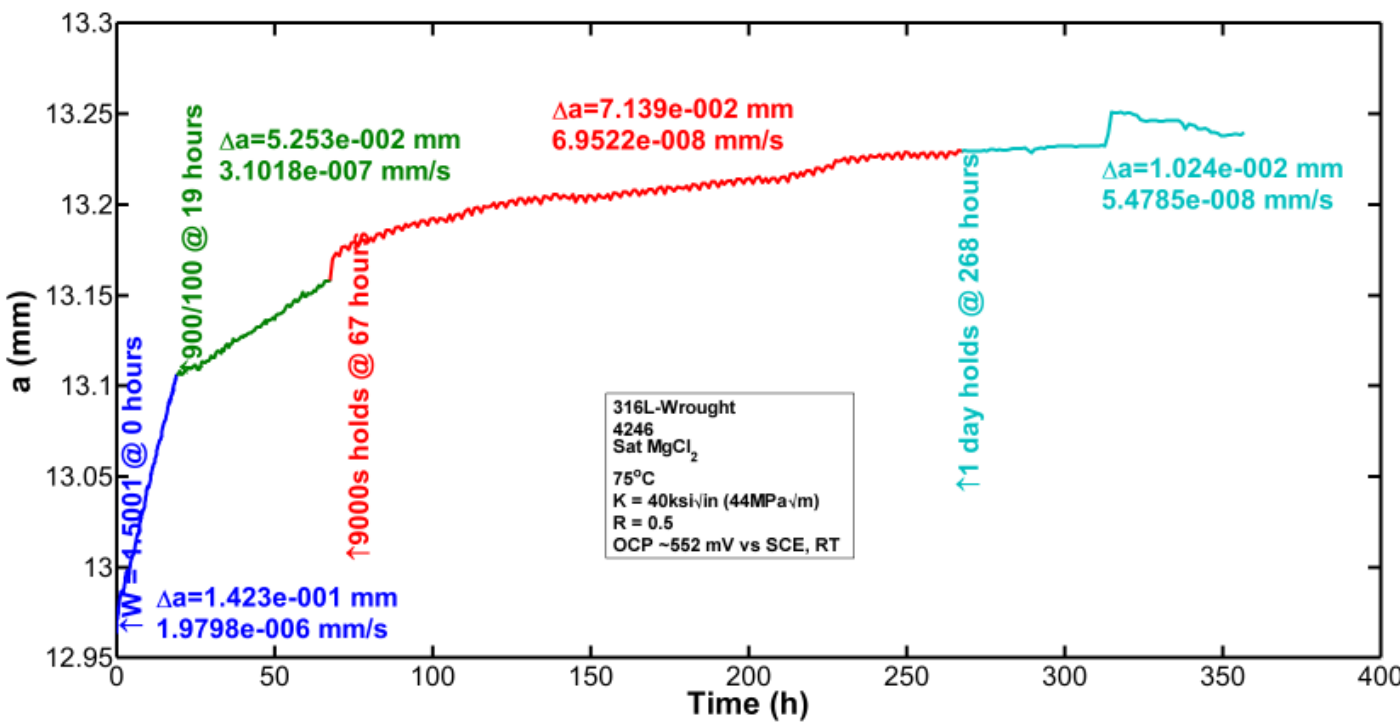
As Received AM sample appears to have a slightly higher E_{corr} compared to the Wrought/1200C-2h samples.

Full test sequence for DCPD measurements



Crack length and corrosion potential measurement over the course of entire experiment on wrought 316L in saturated $MgCl_2$ at 75°C.

Crack Growth Rate – 316L Wrought

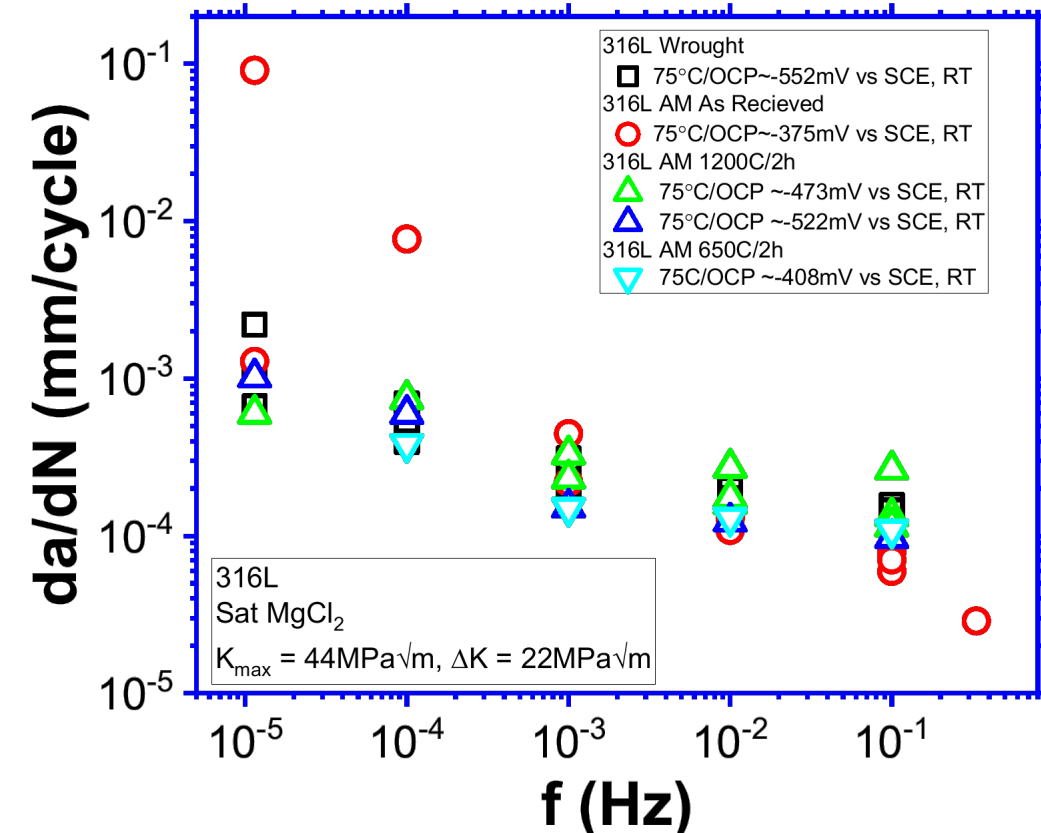
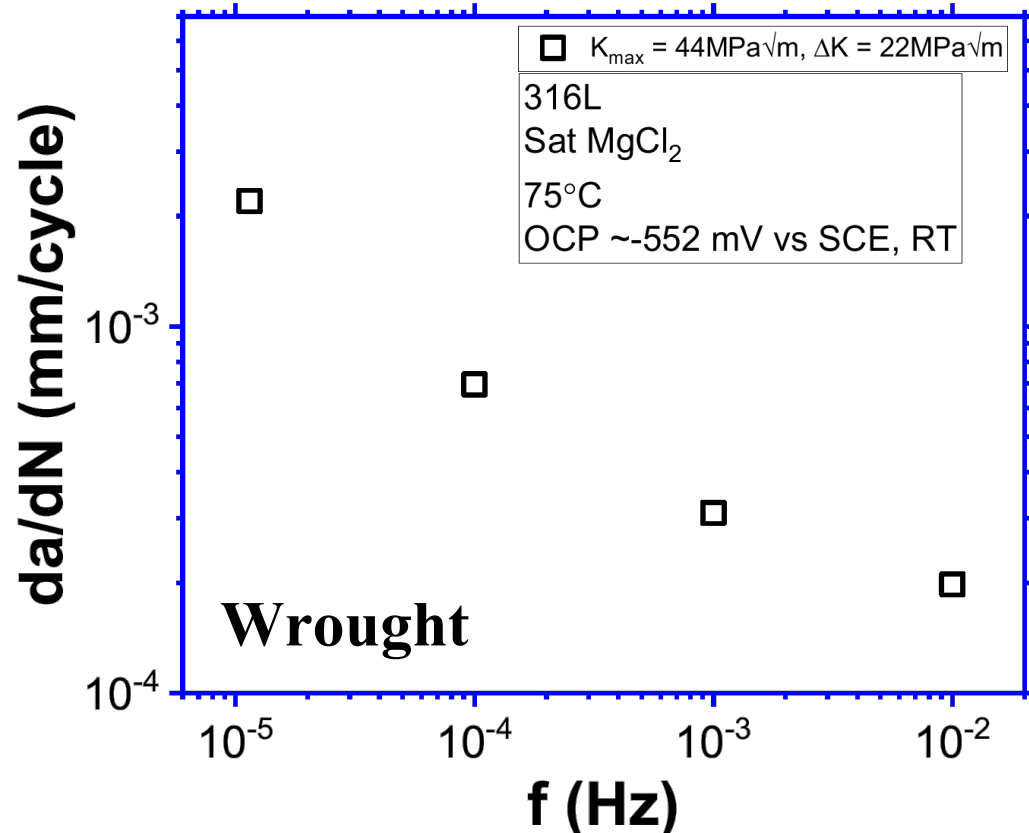


Measurements are performed in saturated MgCl_2 at 75°C (6.4 M).

A $K_{max} = 44 \text{ MPa}\sqrt{\text{m}}$ and a loading ratio, $R = 0.5$ ($\Delta K = 22 \text{ MPa}\sqrt{\text{m}}$) were used to propagate the pre-crack to a constant K condition.

Holds at 9,000 and 86,400 seconds at low frequencies (0.01 and 0.001 Hz) were used to propagate the crack to constant K .

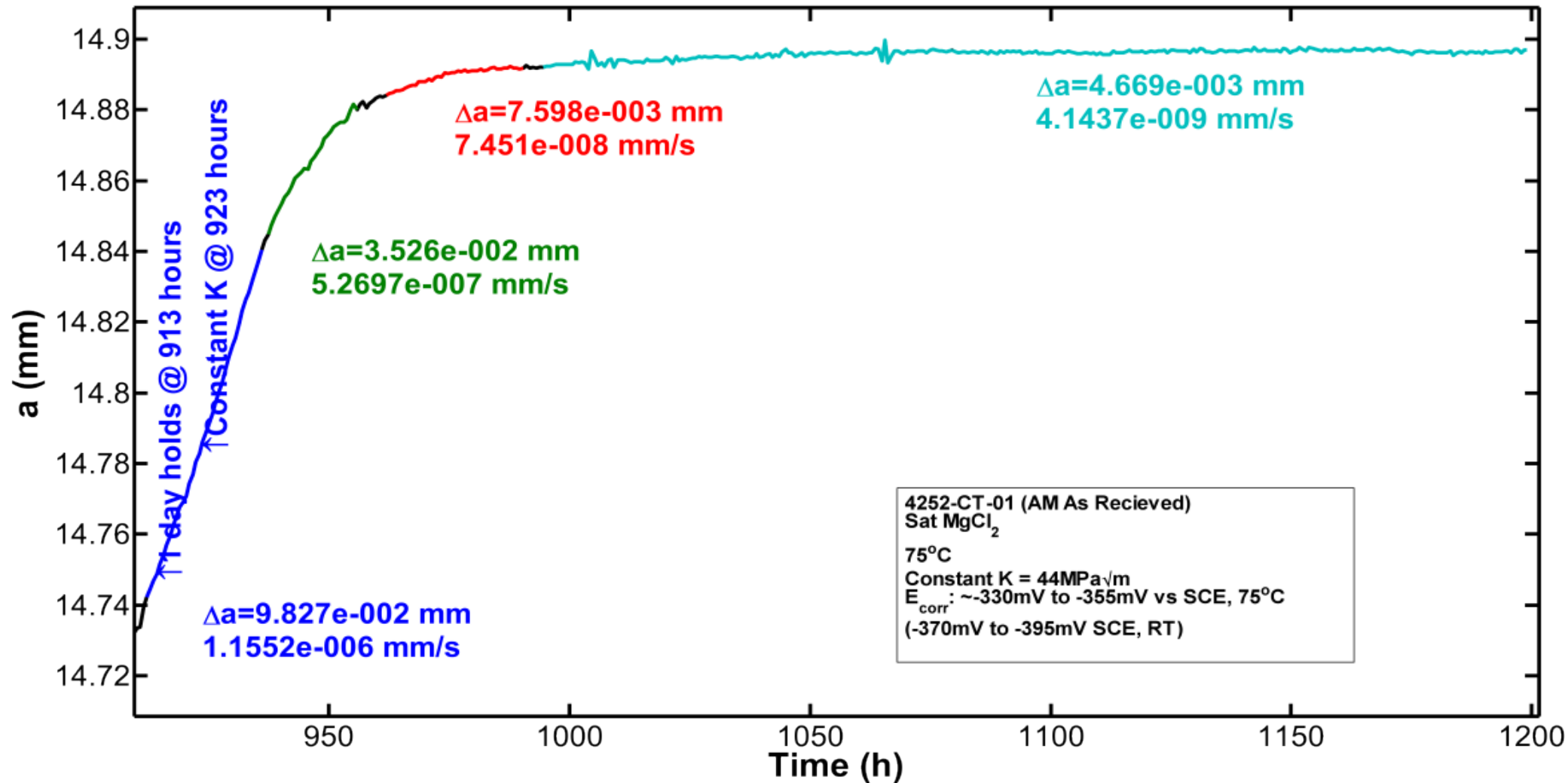
316L – frequency dependency (corrosion fatigue data)

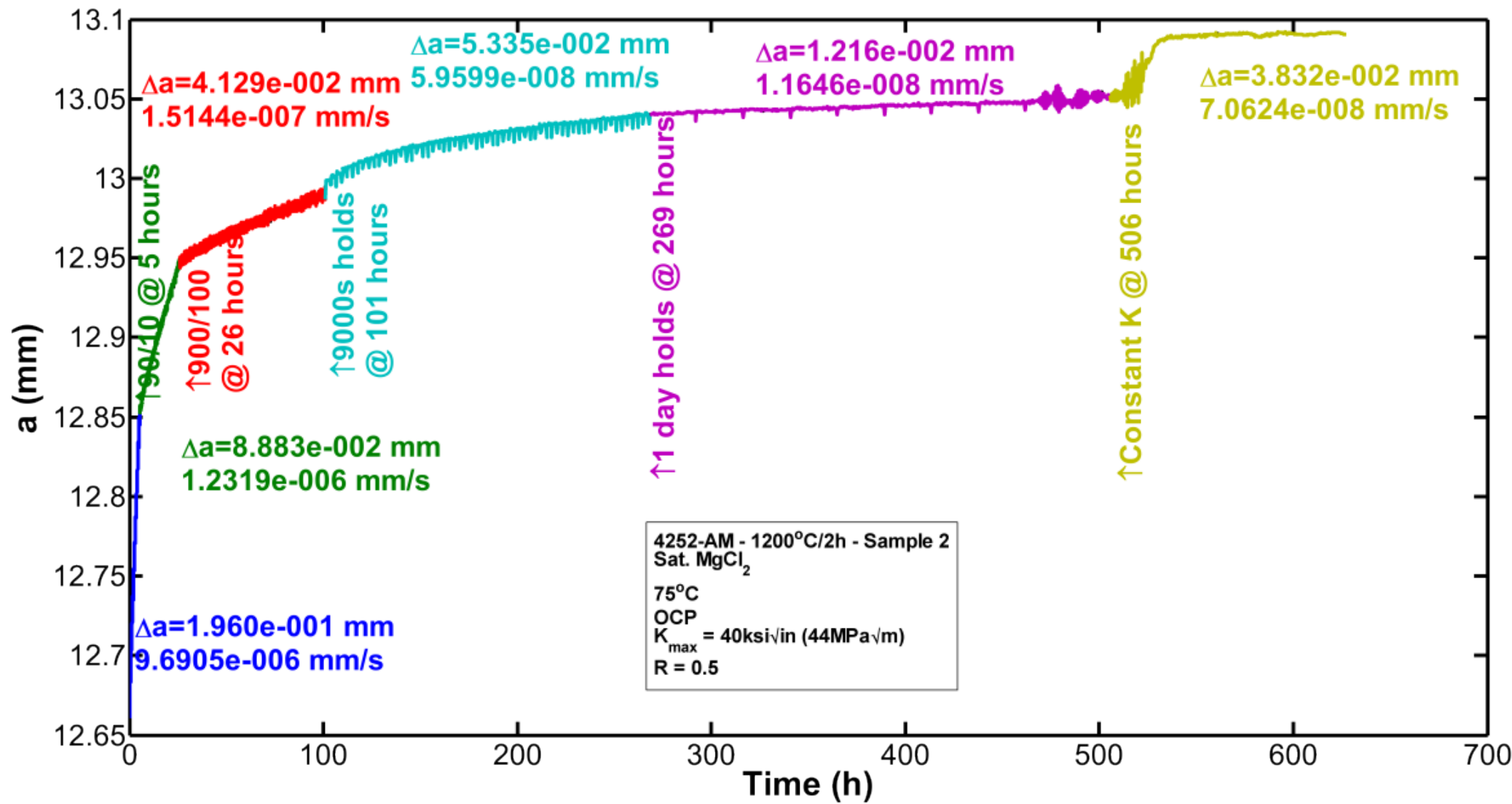


This frequency dependence on crack growth could be caused by an increase in crack tip anodic dissolution:

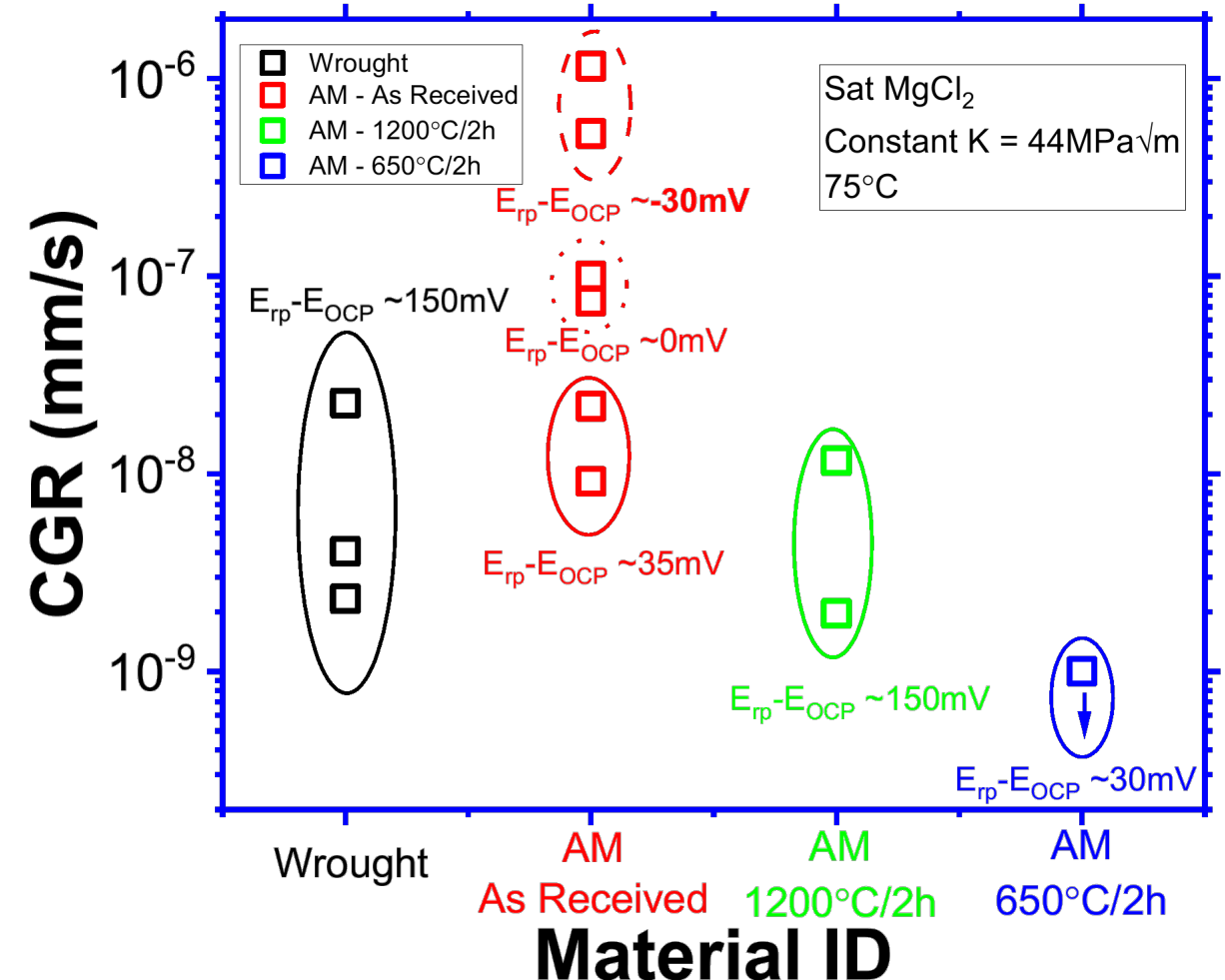
- (1) increase local cathodic production of embrittling hydrogen; and
- (2) lead to further crack tip acidification through hydrolysis of dissolved metal ions.

316L-AM As-printed – crack growth rate (CGR)





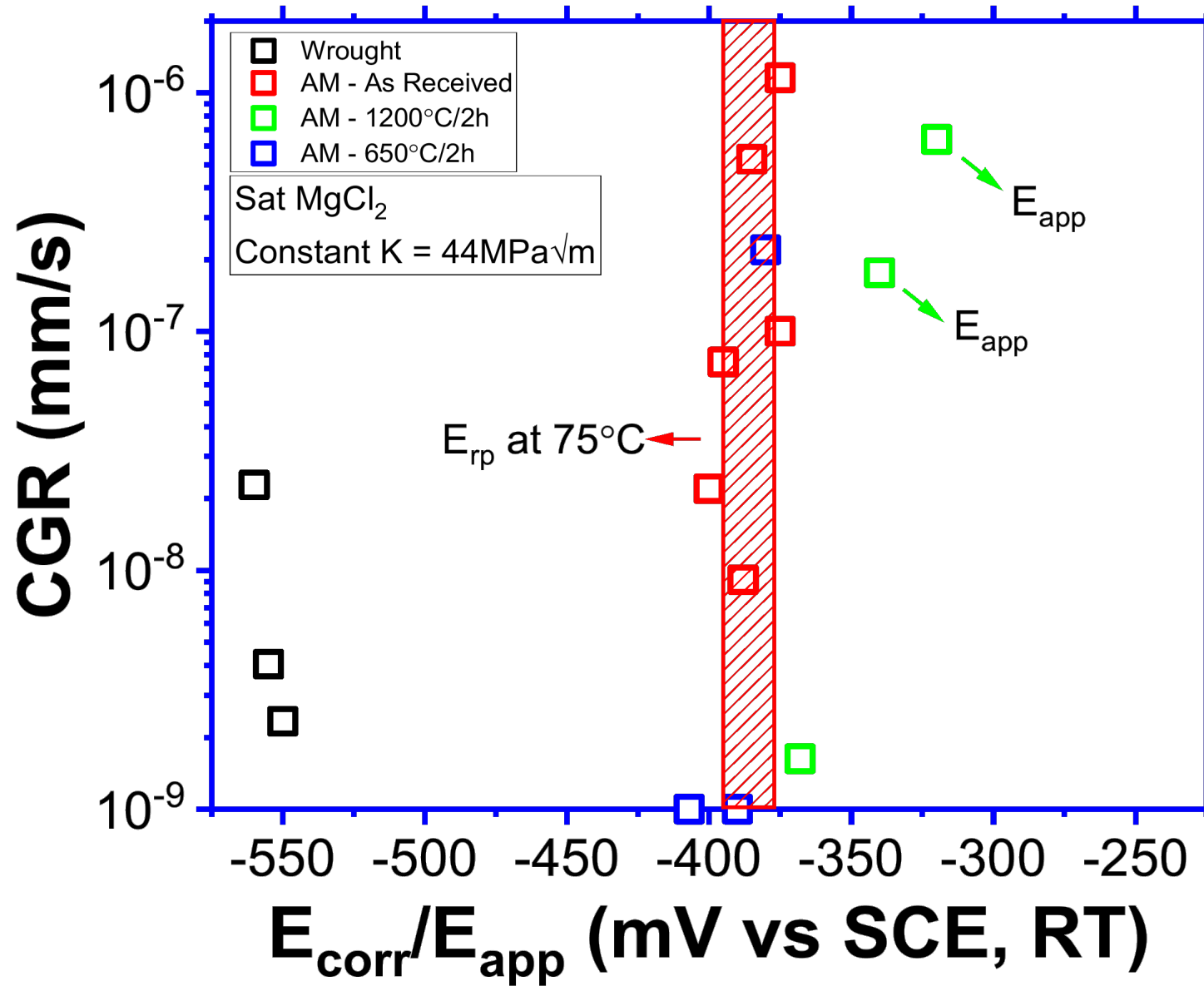
Constant K



Constant K behavior established for different 316L conditions:

- 316L – AM As received sample exhibits the highest values of CGR.
 - Seems to be associated with high OCP values – still flushing this out.
- CGR is low $\sim 10^{-8}$ mm/s when $E_{OCP} < E_{rp}$ in all cases.
- CGR is in the range of 10^{-7} mm/s when $E_{OCP} \sim E_{rp}$ and is about 10^{-6} mm/s when $E_{OCP} > E_{rp}$.

CGR potential relationship with E_{rp}



Conclusions/open questions on AM SCC:

- Evidence of environmental effects at 75°C. This frequency dependence on crack growth could be caused by an increase in crack tip anodic dissolution.
- CGR of annealed AM and wrought material were consistently between 10^{-8} and 10^{-7} mm/sec.
 - As-printed material showed more fluctuations (10^{-8} to 10^{-6} mm/sec).
- Appeared to be a correlation between E_{OCP} relative to E_{RP} and CGR.

Impact of microstructure on crack path still needs to be addressed:

- What path will SCC take?
 - Sub-grain boundaries?
 - Melt pool boundaries? – Boiling MgCl₂ suggests these have minimal impact.
 - High angle grain boundaries?
- Residual stress effects?
 - Making these measurements now.
- Non-metallic inclusion effects?
 - Same as in water reactor studies?
 - Heat treatments might have an impact on this as well, oxide inclusion coarsening.

Inherent Strain Method for Rapid Stress Prediction



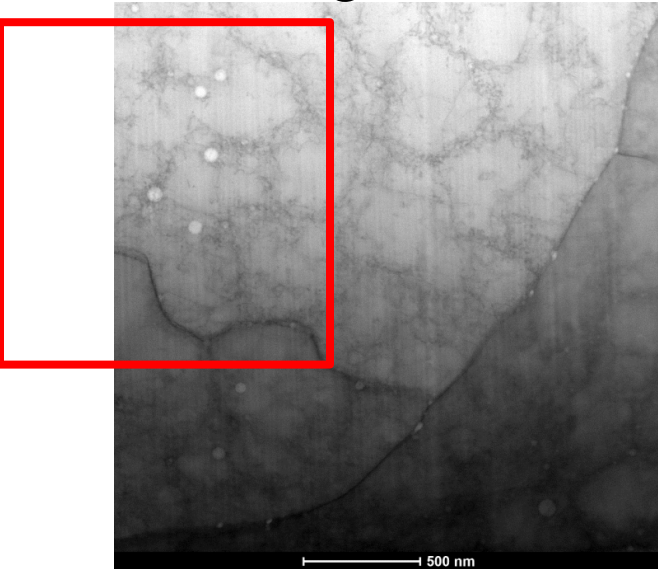
- Large LPBF part size is challenging for full thermomechanical solution due to small, fast moving laser
 - Minimum simulation timestep is typically $\frac{r_{laser}}{v_{laser}}$, where r is the laser radius and d is the laser diameter. For typical ProX 200 settings, this is a timestep of roughly 3.5e-5 s for builds that may take hours or days.
- Inherent strain method originally developed for weld stress prediction
 - (Ueda, Fukuda, Tanigawa 1979; Ueda, Kim, Yuan 1980, Hill and Nelson 1995)
 - Recently extended to AM (Chen et al. 2019, Liang et al. 2019 & 2020)
- Strain tensor is applied in layers over time in a purely mechanical simulation
 - Quick approximation for distortion and stress

$$\bar{\varepsilon} = \begin{bmatrix} \varepsilon_{11} & 0 & 0 \\ 0 & \varepsilon_{22} & 0 \\ 0 & 0 & \varepsilon_{33} \end{bmatrix}$$

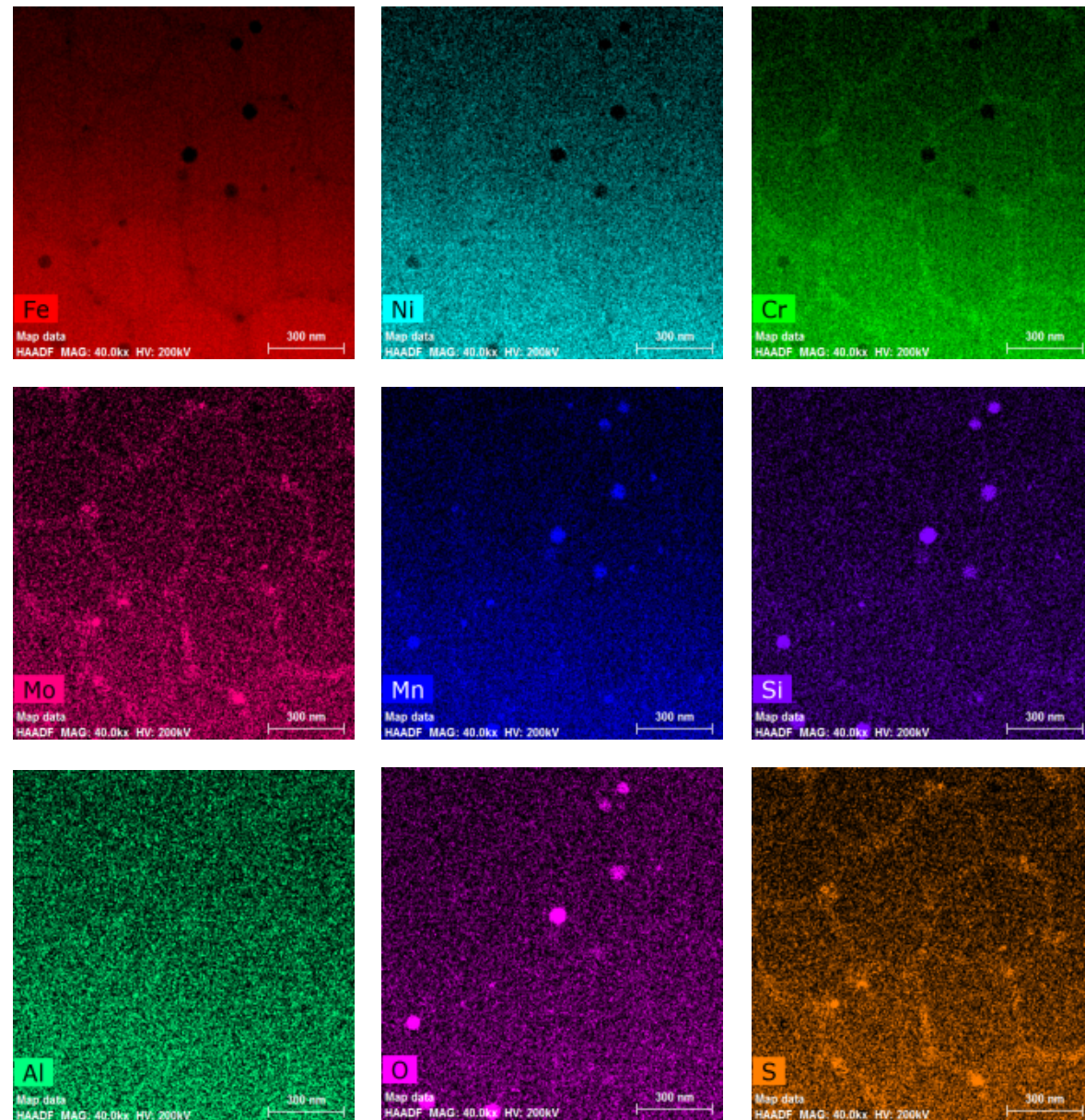
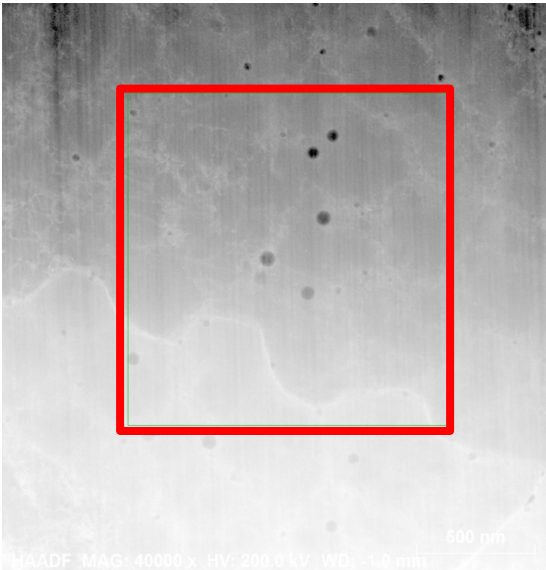
- Does not capture local variations due to different thermal gradients
- Fast due to layer-based approach and only mechanical solve
- Employed in Sandia's Sierra/SolidMechanics FEA code

As-printed microstructure – STEM/EDS

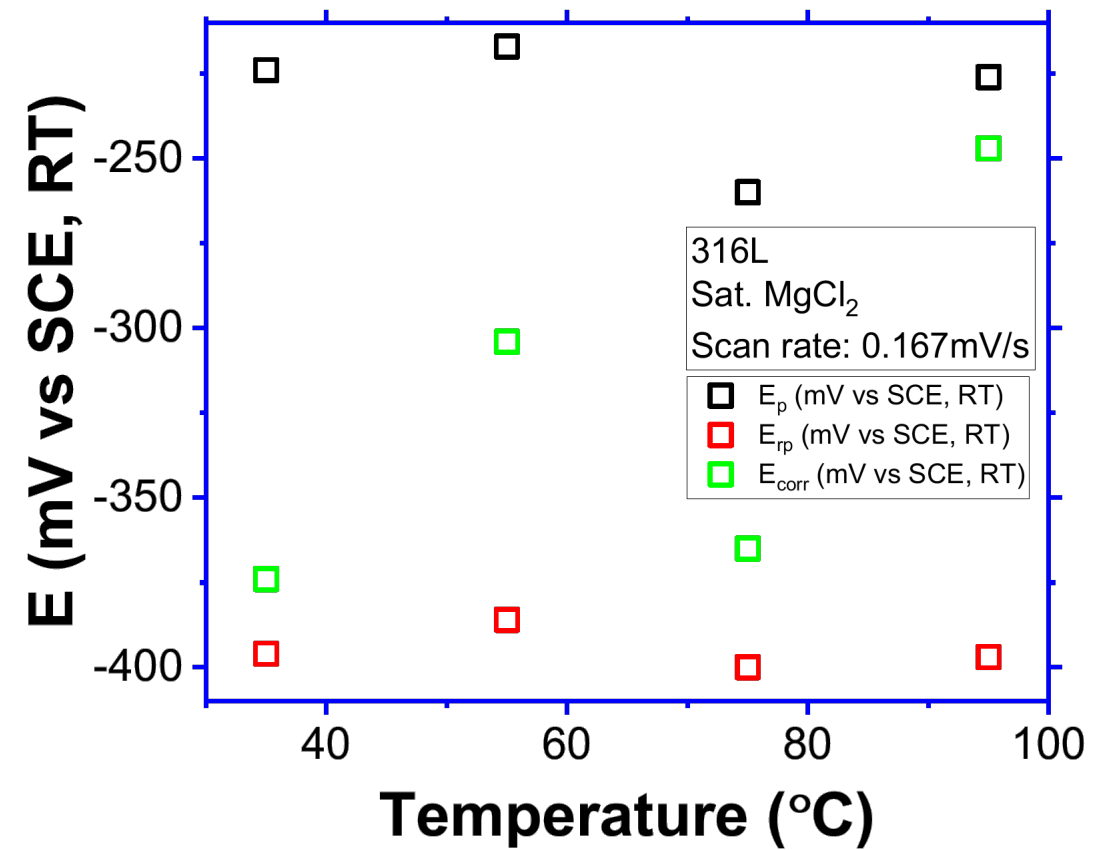
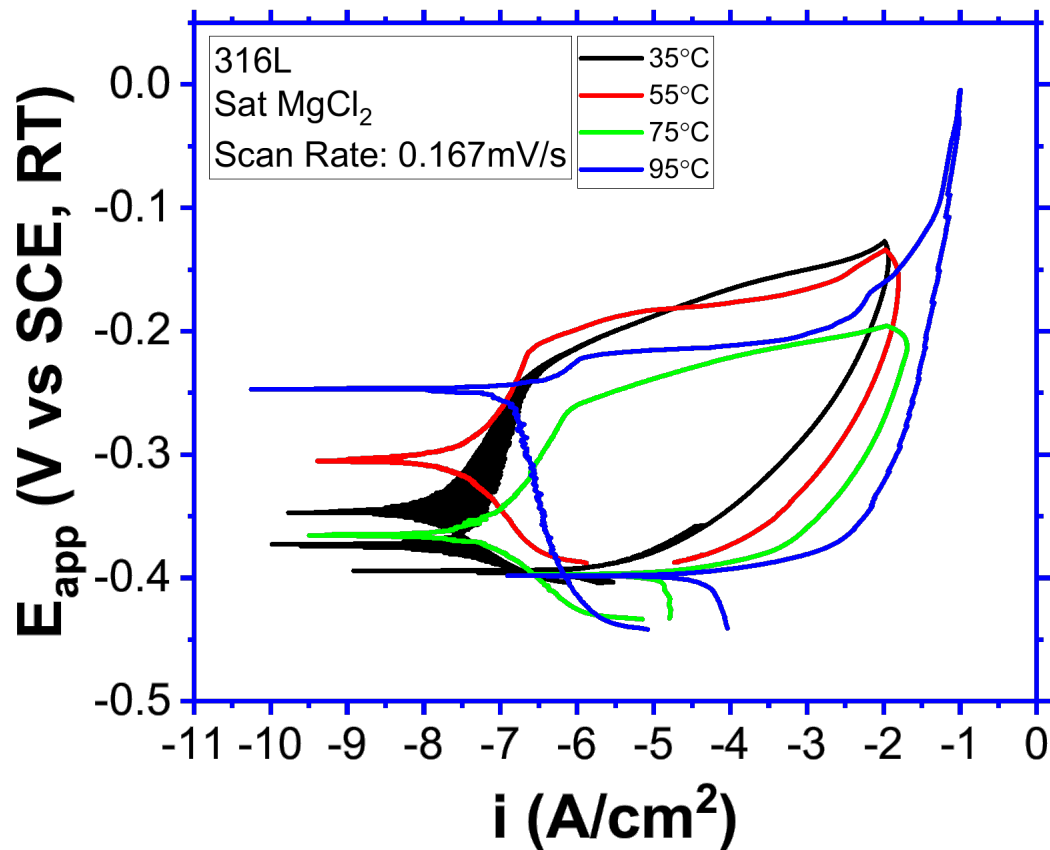
Bright field



Dark field



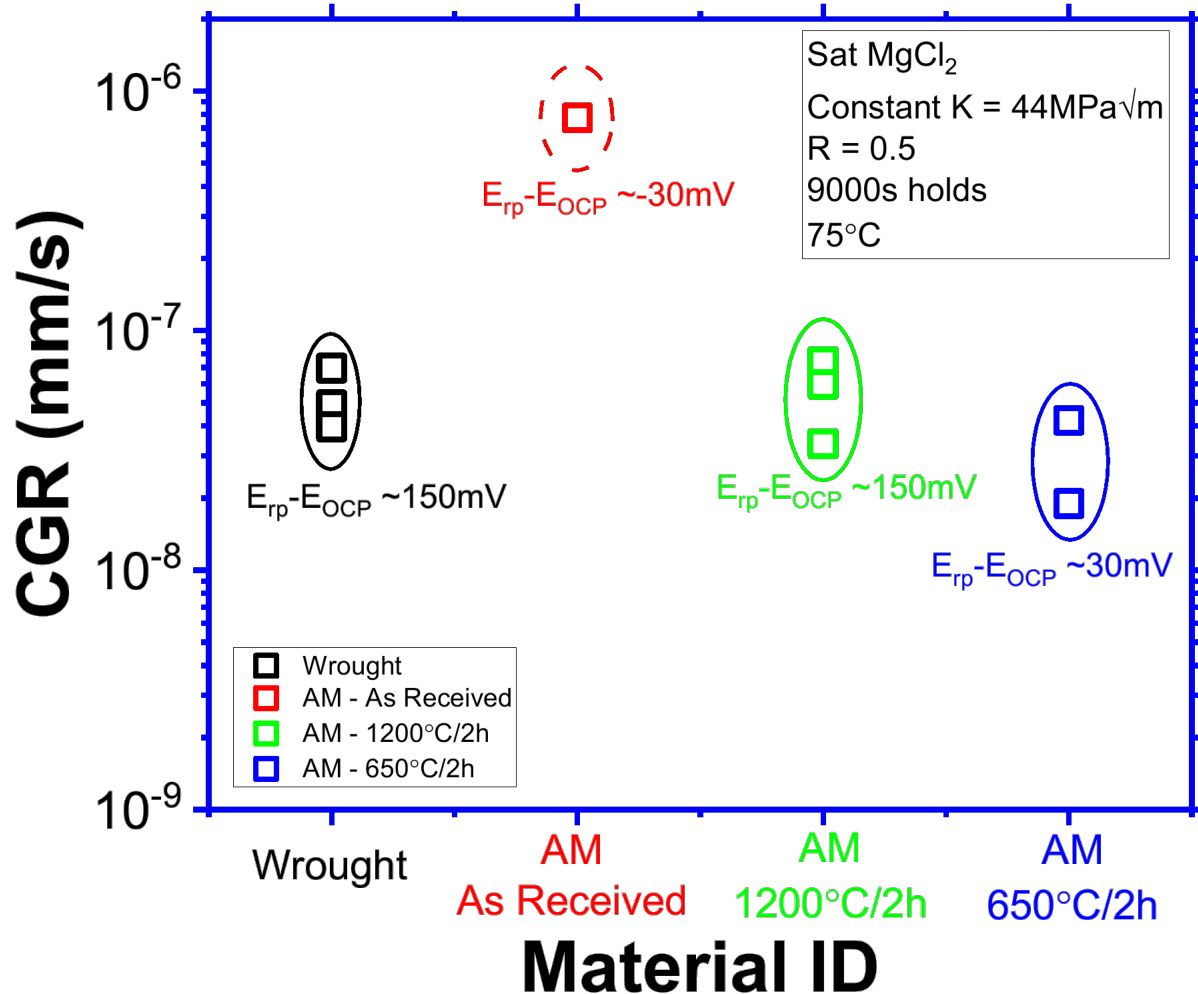
Electrochemical Tests – Sat. MgCl₂



No significant effect on E_p or E_{rp} with temperature

E_{corr} at 95°C is close to E_p and is a significant increase above E_{rp}

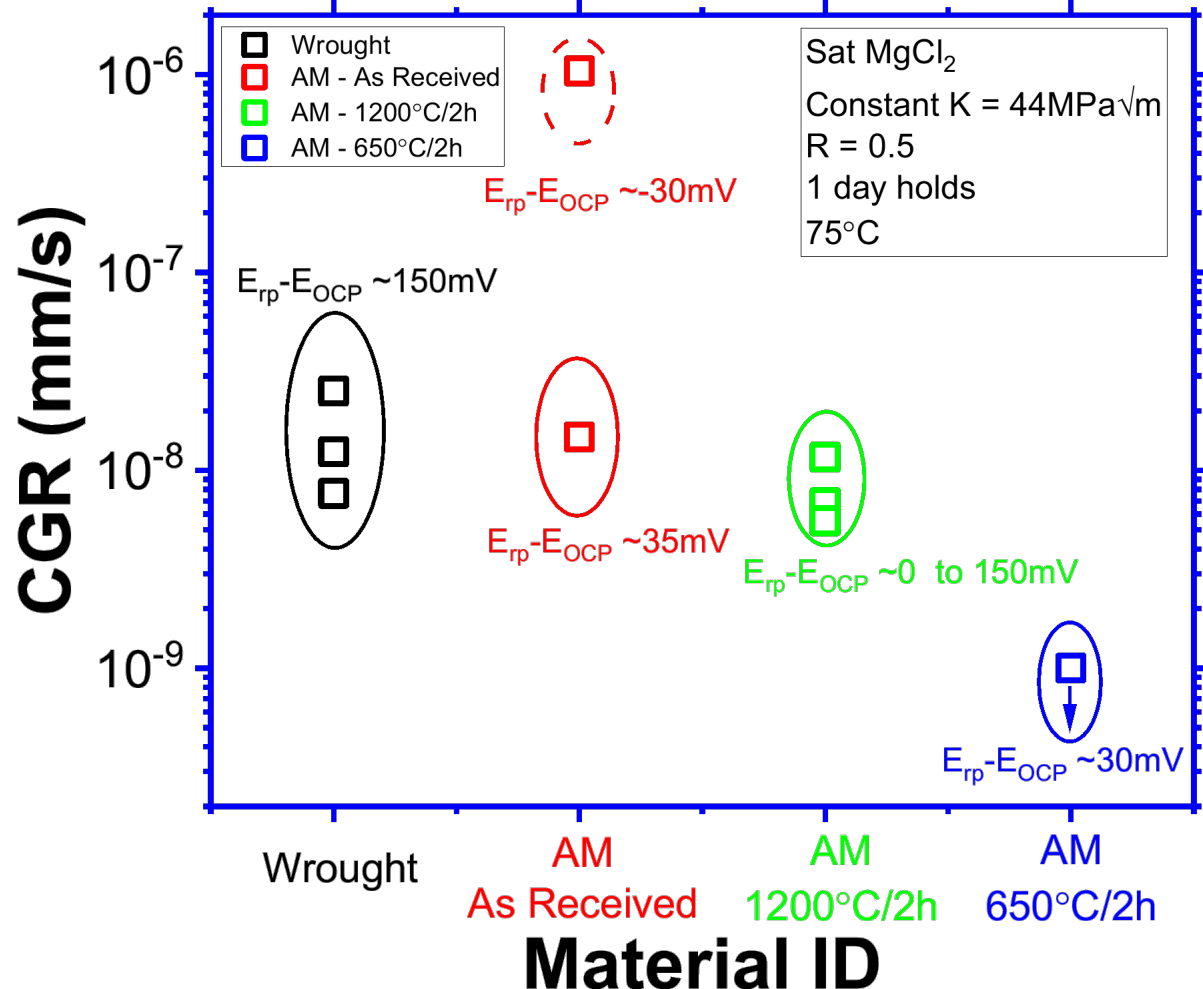
Constant K – 9000s Holds



Constant K – 9000s holds behavior for different 316L conditions

- 316L – AM As received sample exhibits the highest values of CGR primarily associated with high OCP values.
- CGR is low $\sim 3-6 \times 10^{-8}$ mm/s when $E_{OCP} < E_{rp}$ in all cases
- CGR is in the range of about 10^{-6} mm/s when $E_{OCP} > E_{rp}$

Constant K – 1 day Holds



Constant K – 1 day holds behavior for different 316L conditions

- 316L – AM As received sample exhibits the highest values of CGR primarily associated with high OCP values.
- CGR is low $\sim 10^{-8}\text{mm/s}$ when $E_{OCP} < E_{rp}$ in all cases
- CGR is in the range of about 10^{-6} mm/s when $E_{OCP} > E_{rp}$